

Similar ratios of introns to intergenic sequence across animal genomes

Warren R. Francis¹ Gert Wörheide^{1,2,3}

(1) Department of Earth and Environmental Sciences, Paleontology and Geobiology, Ludwig-Maximilians-Universität München, Richard-Wagner Straße 10, 80333 Munich, Germany

(2) GeoBio-Center, Ludwig-Maximilians-Universität München, Munich, Germany

(3) Bavarian State Collection for Paleontology and Geology, Munich, Germany

Keywords: metazoa, comparative genomics, junk DNA, complexity, C-value

Abstract

One central goal of genome biology is to understand how the usage of the genome differs between organisms. Our knowledge of genome composition, needed for downstream inferences, is critically dependent on gene annotations, yet problems associated with gene annotation and assembly errors are usually ignored in comparative genomics. Here we analyze the genomes of 68 species across 12 animal phyla and some single-cell eukaryotes for general trends in genome composition and transcription, taking into account problems of gene annotation. We show that, regardless of genome size, the ratio of introns to intergenic sequence is comparable across essentially all animals, with nearly all deviations dominated by increased intergenic sequence. Genomes of model organisms have ratios much closer to 1:1, suggesting that the majority of published genomes of non-model organisms are underannotated and consequently omit substantial numbers of genes, with likely negative impact on evolutionary interpretations. Finally, our results also indicate that most animals transcribe half or more of their genomes arguing against differences in genome usage between animal groups, and also suggesting that the transcribed portion is more dependent on genome size than previously thought.

Introduction

Understanding why genomes vary greatly in size and how organisms make different use their genomes have been central questions in biology for decades [1]. For many bacteria, the majority of the genome is composed of relatively short genes, averaging around 1000bp, and coding for proteins. Indeed, the largest bacterial genome (a myxobacterium) that has been sequenced is only 14 megabases, containing an estimated 11,500 genes [2]. However, for eukaryotic organisms, genomes can be over ten-thousand-fold larger than bacterial genomes due to an increase in the number of genes (tens of thousands compared to a few thousand in most bacteria), expansion of the genes themselves due to the addition of introns, and expansion of the sequence between genes.

As the number of genome projects has grown, massive amounts of data have become available to study how organisms organize and use their genomes. Genome projects vary substantially in quality of assembly and annotation [3,4]. Unfortunately, the predicted genes are often taken for granted as being correct when these are only hypotheses of gene structure [5]. For example, one study found that almost half of the genes in the *Rhesus* monkey genome had a predictable annotation error when compared to the closest human homolog [6]. This has profound implications for all downstream analyses, such as studying evolution of

41 orthologous proteins [7] and phylogeny based on protein matrices or gene content [8,9]. When considered
42 across all genes, systematic errors in genome assembly or annotation would severely skew bulk parameters
43 of a genome.

44
45 While issues of assembly are often thought to be technical problems that are resolved before continuing,
46 all subsequent analyses are dependent upon accurate genome assembly and annotation. The absence of a
47 protein family in a particular organism is only meaningful if it is certain that it is absent from the genome
48 and not merely the annotation, therefore it is of utmost importance that all genes are properly represented.
49 Yet for most genome projects of non-model organisms, there are limited methods to determine if the assem-
50 bly and annotation are sufficient for downstream comparative analyses. Internal metrics can be used, such
51 as the fraction of raw genomic reads or ESTs that map back to the assembly, though this does not tell us if a
52 gene is believable in the context of other animals. Alternatively, counts of “universal” single-copy orthologs
53 have been proposed as a metric of genome completeness [10,11], though these genes only represent a small
54 subset of all genes (few hundred out of tens of thousands in most animals).

55
56 Identification of universal trends in genome organization and transcription may enable better quantita-
57 tive metrics of genome completeness. Mechanistic models relating to evolution of gene content or coding
58 fractions tended to focus on bacteria or archaea because of the relative ease of annotation. In regards to
59 eukaryotes, some patterns in genome size have been discussed [12–14]. Additionally, a handful of studies
60 have analyzed genome size in connection to other parameters such as indels [15], transposon content [16–19],
61 average intron length [20,21] or total intron length [18]. Despite these advances, none of these studies have
62 estimated the amount of the genome that is genic (exonic plus intronic, including non-coding) based on in-
63 dependent examination of single genomes and without averaging over a whole kingdom. Additionally, none
64 of them have described a way to account for technical problems in assembly and annotation.

65
66 Here we examine basic trends of genome size and the relationship to annotation quality across animals
67 and some single-celled eukaryotes. We show that assembly and annotation errors are widespread and pre-
68 dictable and that many genomes are likely to be missing many genes. We further show that re-annotation
69 of select species with publicly available tools and transcriptome data improves the annotation. Future users
70 may benefit if databases incorporate more recent data from transcriptome sequencing, and update annota-
71 tion versions more frequently. Comparison of genomic composition across many animal groups indicated a
72 ratio of introns:intergenic approaching 1:1, suggesting this as a potential parameter to identify genome com-
73 pleteness across metazoans, and potentially other eukaryotes. Finally, this implies that animals transcribe
74 at least half of their genomes whereby small, exon-rich genomes transcribe most of the genome and large
75 genomes transcribe approximately half of the genome.

77 Methods

78 Genomic data sources

79 Data sources and parameters are available in Supplemental Table 1.

80
81 Genomic scaffolds and annotations for *Ciona intestinalis* [22], *Branchiostoma floridae* [23], *Trichoplax ad-*
82 *herens* [24], *Capitella teleta* [25], *Lottia gigantea* [25], *Helobdella robusta* [25], *Saccoglossus kowalevskii* [26],
83 *Monosiga brevicollis* [27], *Emiliania huxleyi* [28], and *Volvox carteri* [29] were downloaded from the JGI
84 genome portal.

85
86 Genome assemblies and annotations for *Sphaeroforma arctica*, *Capsaspora owczarzaki* [30] and *Salpin-*
87 *goeca rosetta* [31] were downloaded from the Broad Institute.

88
89 GFF annotations v2.1 [32] for *Amphimedon queenslandica* were downloaded from the Amphimedon
90 Genome website (<http://amphimedon.qcloud.qcif.edu.au/downloads.html>), and v1 annotations [33] and as-
91 semblies were downloaded from Ensembl.

92
93 For *Nematostella vectensis*, Nemve1 assembly and annotations [34] were downloaded from JGI, and the
94 transcriptome for comparative reannotation was downloaded from <http://www.cnidariangenomes.org/> [35].
95

96 Genome assembly, transcriptome assemblies from Cufflinks and Trinity, and GFF annotations for *Mne-*
97 *miopsis leidy* [8] were downloaded from the Mnemiopsis Genome Portal (<http://research.nhgri.nih.gov/mnemiopsis/>).
98 Assembly and annotations for *Sycon ciliatum* [36] were downloaded from COMPAGEN. Assembly and
99 annotation for *Botryllus schlosseri* [37] were downloaded from the Botryllus Schloseri genome project
100 (<http://botryllus.stanford.edu/botryllusgenome/>). Assembly and annotation for *Exaiptasia pallida* (for-
101 merly *Aiptasia sp.*) [38] were downloaded from <http://reefgenomics.org>. Assembly and annotation for *Oiko-*
102 *pleura dioica* [39] were downloaded from Genoscope (<http://www.genoscope.cns.fr/externe/GenomeBrowser/Oikopleura/>).
103 Assembly and annotation for *Tetrahymena thermophila* were downloaded from the Tetrahymena Genome
104 Database (ciliate.org). Assembly and annotation for *Symbiodinium kawagutii* [40] were downloaded from
105 the Dinoflagellate Resources page (web.malab.cn/symka_new/index.jsp).
106

107 Assemblies and annotations for *Symbiodinium minutum* [41], *Pinctada fucata* [42], *Acropora digitifera*
108 [43], *Lingula anatina* [44], *Ptychodera flava* [26], and *Octopus bimaculoides* [45] were downloaded from the
109 OIST Marine Genomics Browser (<http://marinegenomics.oist.jp/gallery/>).
110

111 Builds of *Homo sapiens*, *Pan troglodytes*, *Mus musculus*, *Canis lupus* [46], *Monodelphis domestica* [47],
112 *Ornithorhynchus anatinus* [48], *Xenopus tropicalis* [49], *Struthio camelus* [50], *Gallus gallus*, *Taeniopygia*
113 *guttata* [51], *Aptenodytes forsteri* [50], *Anas platyrhynchos* [52], *Melopsittacus undulatus* [53], *Alligator mis-*
114 *sissippiensis* [54], *Anolis carolinensis* [55], *Chrysemys picta bellii* [56], *Chelonia mydas* [57], *Pelodiscus*
115 *sinensis* [57], *Python bivittatus* [58], *Salmo salar*, *Danio rerio* [59], *Latimeria chalumnae* [60], *Petromy-*
116 *zon marinus* [61], *Callorhynchus milii* [62], *Crassostrea gigas* [63], *Dendroctonus ponderosae* [64], *Tribolium*
117 *castaneum* [65], *Bombyx mori* [66], *Limulus polyphemus* [67] were downloaded from the NCBI Genome server.
118

119 Genome assemblies and annotations of *Caenorhabditis elegans* [68], *Drosophila melanogaster*, *Strongy-*
120 *locentrotus purpuratus* [69], *Daphnia pulex* [70], *Apis mellifera* [71], *Ixodes scapularis* [72], *Strigamia mar-*
121 *itima* [73] were downloaded from Ensembl.
122

123 Calculation of exonic and genic sequence

124 For all analyses, we used the total number of bases in the downloaded assembly as the total genome size,
125 bearing in mind that this may result in a systematic underestimation of total genome size as repeated regions
126 may be omitted from assemblies. For example, the horseshoe crab *L. polyphemus* has a scaffold assembly of
127 1.8Gb while the reported genome size is 2.7Gb [67], a difference of almost a gigabase.
128

129 If GFF format files were available for download with a genome project, or on databases (Ensembl or
130 NCBI), those were used preferentially. The analysis procedure is described in Fig 1. Total base pairs of
131 exon, intron, intergenic, and gaps were counted from each GFF file and genomic contigs (or scaffolds) with
132 a custom Python script (gtfstats.py, available at bitbucket.org/wrf/sequences). For calculations of exonic or
133 genic bases, the script converts all gene and exon annotations to intervals and ignores the strand. Here, gene
134 (or genic) is defined as transcribed bases that are either exon or intron, regardless of coding potential. All
135 overlapping exon intervals are merged, meaning that alternative splice sites, or exons on the opposite strand,
136 are treated as a single interval for bulk calculations. The same is done for genes or transcripts, whichever is
137 available. Introns are calculated as the difference of the genic set and the exonic set, as introns are typically
138 not defined as separate features in normal GFF files. This means that any sequence that is an exon on one
139 strand and an intron on the other is treated for these calculations as an exon, meaning those base or their
140 reverse complement (hence base pairs) are transcribed and retained following splicing in some case (Fig 1D
141 and E). Intergenic sequence is defined as the difference between total sequence base pairs and genic base
142 pairs, and gaps are defined as any repeats of 'N's longer than one base.
143

144 If exons are not specified, then coding sequences (CDS) are used instead if they are available, such as
145 for AUGUSTUS predictions. Additional non-coding features such as “microRNA”, “tRNA”, “ncRNA” are
146 included for gene and exon calculations if they were in the standard GFF3 format. Some genomes made use
147 of mapped RNAseq data, which implicitly included all non-coding RNAs as well. Some annotations had to
148 determine the gene ID from the exons. For example, most of the GTF files from the earlier JGI genomes
149 had only exons annotated, without individual features for genes or mRNAs, so the gene was then defined as
150 all of the exons with the same feature ID even though a specific gene feature was undefined.

151
152 Exons defined as part of a “pseudogene”, or genes defined as pseudogenes, were also excluded from all
153 counts. We justify this because pseudogenes are subject to problems of definitions and population sampling
154 bias. Pseudogenes are defined as having the appearance or structure of normal protein coding genes, in-
155 dependent of transcriptional potential, but that would be unable to produce a functional protein, perhaps
156 through nonsense mutations. Therefore, a pseudogene that is transcribed and cannot code for a protein
157 should be annotated as a “transcribed pseudogene”, though potentially could be a non-coding RNA. Pseu-
158 dogene features are not annotated for all species, making it difficult to compare broadly. Additionally, for
159 most non-model species, the genomes are generally based upon a single individual rather than a reference for
160 a population based on a large number of individuals. Therefore, if that single individual were homozygous for
161 a nonsense mutation but other individuals in the population were not, that gene should not be a pseudogene.

162
163 All downstream correlation calculations and graphs were done in R. Regression was calculated using the
164 “lm()” function, for linear ($y \sim x$), exponential ($\log(y) \sim x$), or hyperbolic ($y \sim 1/x$) models, and the “predict()”
165 function was used to model curves. The raw data table and the R source code used to generate figures is
166 available at bitbucket.org/wrf/genome-reannotations.

168 Calculation of average exon and intron length

169 The same script (`gtfstats.py`, available at bitbucket.org/wrf/sequences) also calculated the average exon and
170 intron length, though these were analyzed separately. All non-redundant exons for all splice variants were
171 taken into account for determination of averages. Unlike the total base pair calculations, genes are separated
172 by strand. Identical exons of splice variants were treated as one exon and counted once, however, alternative
173 boundaries were treated as a separate exons. Retained introns are treated as exons, not introns. Exon
174 lengths were counted per non-redundant exon for each gene, summed across all genes and divided by the
175 number of non-redundant exons across all genes. The sum of exon lengths for the average length calculation
176 does include redundant bases from antisense transcripts or splice variants, meaning bases from antisense
177 transcripts and alternative-boundary splice variants can be double-counted. Introns were calculated as the
178 space between exons, calculated by gene.

180 Reannotation of select species

181 Due to unexpectedly high or low gene content, six genomes were selected for reannotation.

182
183 The original Triad1 scaffolds of *T. adherens* [24] were reannotated with AUGUSTUS v3.0.3 [74] with
184 the following options: `-strand=both -genemodel=atleastone -sample=100 -keep_viterbi=true -alternatives-`
185 `from-sampling=true -minexonintronprob=0.2 -minmeanexonintronprob=0.5 -maxtracks=2`. Species train-
186 ing was generated using the Triad1 ESTs with the webAugustus Training server [75].

187
188 The original Monbr1 scaffolds of *M. brevicollis* [27] were reannotated with AUGUSTUS as for *T. adherens*,
189 using the same parameters except trained using the Monbr1 ESTs with the webAugustus Training server [75].

190
191 For the hydrozoan *H. magnipapillata*, the original assembly was downloaded from JGI [76] and a new scaf-
192 fold assembly was downloaded from the FTP of Rob Steele at UC Irvine (at <https://webfiles.uci.edu/resteele/public>).
193 For both cases, the scaffolds were reannotated using TopHat22 v2.0.13 [77] and StringTie v1.0.4 [78] with
194 default options by mapping the reads from two paired-end RNAseq libraries, NCBI Short Read Archive

195 accessions SRR922615 and SRR1024340, derived from whole adult animals.

196

197 For the lancelet *B. floridae*, the Braff1 scaffolds [23] were reannotated using TopHat2 v2.0.13 [77] and
198 StringTie v1.0.4 [78] with default options by mapping the reads from the paired-end RNAseq library, NCBI
199 SRA accession SRR923751, from the adult body.

200

201 For the lamprey *P. marinus*, we were unable to find any annotation as GFF or GTF, so we generated
202 one using TopHat2 v2.0.13 [77] and StringTie v1.0.4 [78] based on the Pmarinus-v7 scaffolds from NCBI and
203 the 16 single-end Illumina libraries from NCBI BioProject PRJNA50489.

204

205 For the octopus *O. bimaculoides*, scaffolds were downloaded from the OIST Marine Genomics plat-
206 form [45], and were reannotated using TopHat2 v2.0.13 [77] and StringTie v1.0.4 [78] with default options
207 by mapping 19 paired-end RNAseq libraries from NCBI BioProject PRJNA285380.

208

209 All reannotations are available for download as GTF or GFF files (see <https://bitbucket.org/wrf/genome-reannotations/downloads>).

210
211

212 Results

213 Overview and organization of data

214 A total of 68 genomes were analyzed, with 59 selected across all major metazoan groups and nine genomes
215 of single-celled eukaryotes. For each group, only select species were taken to avoid having a single group
216 dominate the analysis. For example, over 100 mammalian genomes are available though only six were used
217 including three model organisms (human, mouse, dog), opossum and platypus (for the non-eutherian clades,
218 marsupial and monotreme, respectively) and the chimp, to compare directly to the human annotation. In
219 general, parasites were excluded because they often have unusual biology, such as the single-celled eukaryote
220 *T. brucei*, which is known for its unusual RNA processing [79,80].

221

222 Generally, we refer to small and large genomes as those below and above 500Mb, respectively. The small-
223 est animal genome used in this study is that of the larvacean *Oikopleura dioica* (70Mb), while the largest is
224 that of the opossum *Monodelphis domestica* (3598Mb). This range incorporates an existing selection bias,
225 as some of the public genome sequencing projects selected the animal of their clade based on their known
226 small genomes. Two examples of this are the shark *C. milii* and the pufferfish *T. rubripes*. Yet it must
227 be considered that in terms of genomes, they may not be representative of their clades; many other shark
228 genomes are estimated to be over 10Gb (haploid genome size) [81], such that a shark genome of only 1Gb
229 may not be “normal” for sharks.

230

231 Additionally, not all of the species in the sample were sequenced or annotated with the same method,
232 making direct comparison more challenging. For instance, some of the earlier genomes (such as *Branchios-*
233 *toma floridae* and *Trichoplax adherens*) were annotated only with Sanger ESTs (order of tens of Mb), which
234 were used to train gene prediction algorithms. Because not all genes have features easily captured by the
235 EST training, several different results are expected: some genes are split because internal exons are not
236 properly found or may have misassemblies in the draft genomes; adjacent genes on the same strand are
237 fused; or genes are omitted entirely.

238

239 Connection between annotation and understanding of genomes

240 Genome projects of non-model species usually report protein coding regions of a genome. Broadly, there are
241 two methods of doing this, comparison to other proteins from other genomes and by aligning mRNA from
242 ESTs or RNAseq [3]. In practice, improvements in methods have made it relatively easy to directly predict
243 proteins from the genome sequence. However, untranslated regions (UTRs) are difficult to predict and often

244 require evidence from ESTs or transcriptome sequencing for accurate predictions, and this has implications
245 for our measurements of total exons in each genome. This means that even in a “perfect” genome where
246 all coding genes are correctly predicted by an annotation program (perhaps based on similarity to a related
247 species) that the precise positions and amount of UTR may still be unknown, resulting in an underestimation
248 of the amount of exonic sequence (Fig 1A and B). Because of this, the reliance on coding genes is likely to
249 underestimate the usable fraction of the genome.

250

251 To illustrate this, one may consider a hypothetical eukaryotic genome of 60Mb with 10,000 genes and
252 equal fractions of exons, introns, and intergenic sequence, at 20Mb each. For simplicity, all exons are the
253 same size (in this example, 200bp), so an average gene (with ten-exons) may contain one exon for the 5'-
254 UTR, and one for the 3'- UTR, and the remaining eight exons are coding. Based on the above annotation
255 scheme, 20% of the exonic fraction (those containing the 5' and 3'-UTRs) is missing in the final annotation.
256 Two introns per gene are also missing (the first and last introns), about 18% of the intronic fraction. This
257 would yield a final annotation where exons are predicted as 16Mb (26.6% of the genome) and introns as
258 15.5Mb (25.9% of the genome). This would also indicate that 52.6% of the genome is genes, a substantial
259 underestimation from the actual value of 66.6%.

260

261 However, other systematic errors can result in an overestimation of the genic fraction. If we consider mul-
262 tiple genes on the same strand, in a head-to-tail arrangement, and recall that UTRs are often not predicted,
263 then an exon containing the stop codon with a 3'-UTR may be omitted and the predicted gene may continue
264 into the next gene (Fig 1C). If it is assumed that the majority of coding exons are correctly predicted, then
265 if such predictions were made systematically one may expect that the measured amount of exons does not
266 deviate much from the true exonic fraction. However, because introns are defined as the removed sequence
267 between exons of the same gene, then the sequence between the two genes that should have been defined as
268 intergenic will instead be defined as intronic, thus raising the intron:intergenic ratio above 1.

269

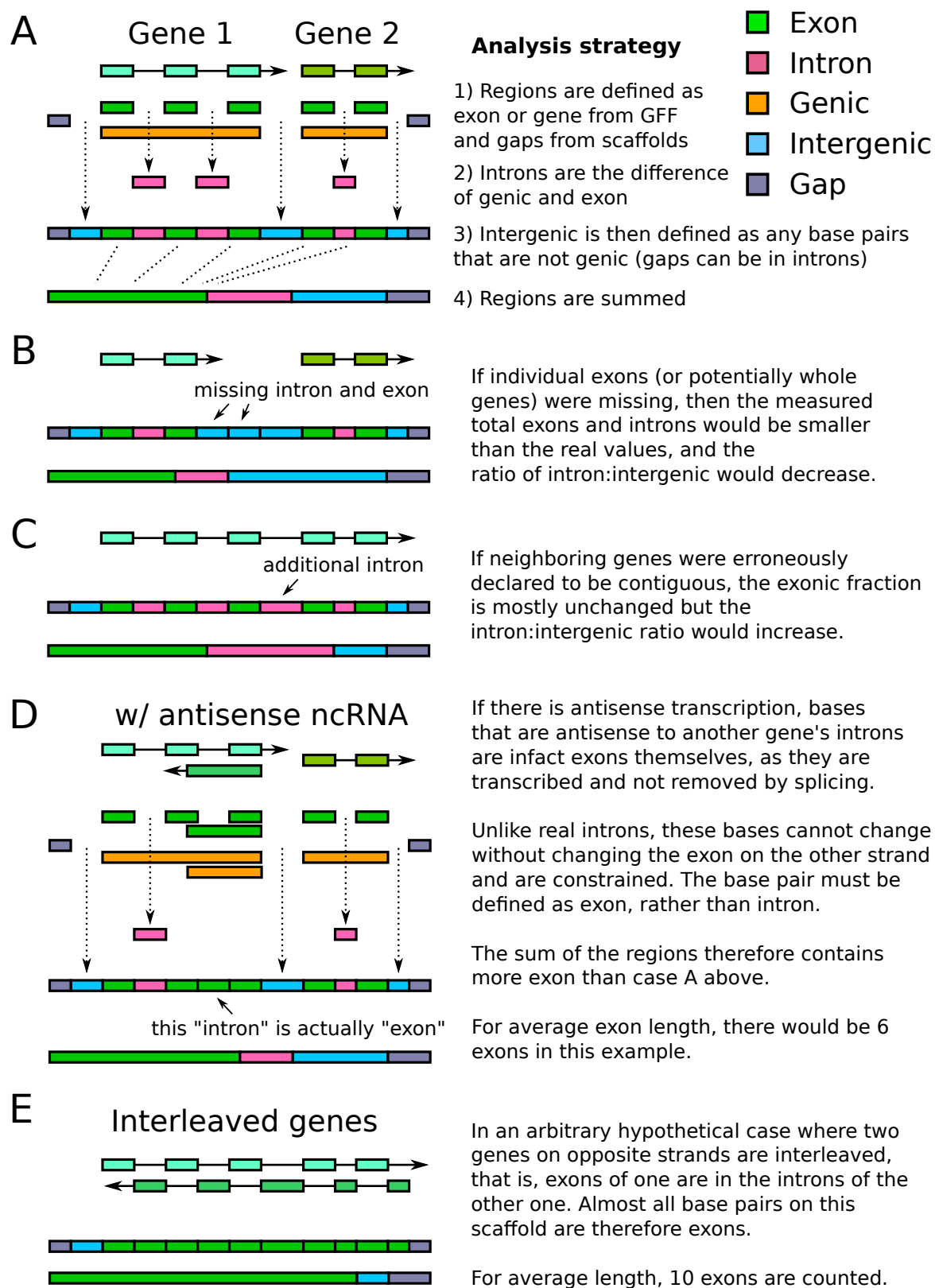


Figure 1: **Schematic of analysis, misannotations and the effects on coding fraction** (A) In a normal case, two hypothetical genes on the same strand are identified. The exons and introns are defined, and the total lengths of those features are summed and displayed in the bars below. Because real genome assemblies can often contain gaps, sample gaps are also shown at the edges of the segment. (B) Case of missing exon or gene annotations, where the intron:intergenic decreases. (C) Case of falsely fused genes, where the intron:intergenic ratio would increase. (D) Case of antisense transcription, where base pairs that are intron on the sense strand and exon on the antisense strand are necessarily defined as exon. (E) Any arbitrary, interleaved genes, or any exons inside of introns, must as well be counted as exon.

270 The above problems assume that the genomic assembly is nonetheless correct, yet the annotation is
 271 directly affected by assembly problems as well. Of the two main sources of problems, repeats [82] and het-
 272 erozygosity [26, 42, 63, 83], repeats often result in breaks in the assembly that could split genes (Fig 2A).
 273 Genes that are split at contig boundaries are likely to have exons missing (or on other scaffolds) and thus
 274 the sequence that should be defined as introns would be instead defined as intergenic (Fig 2B).
 275

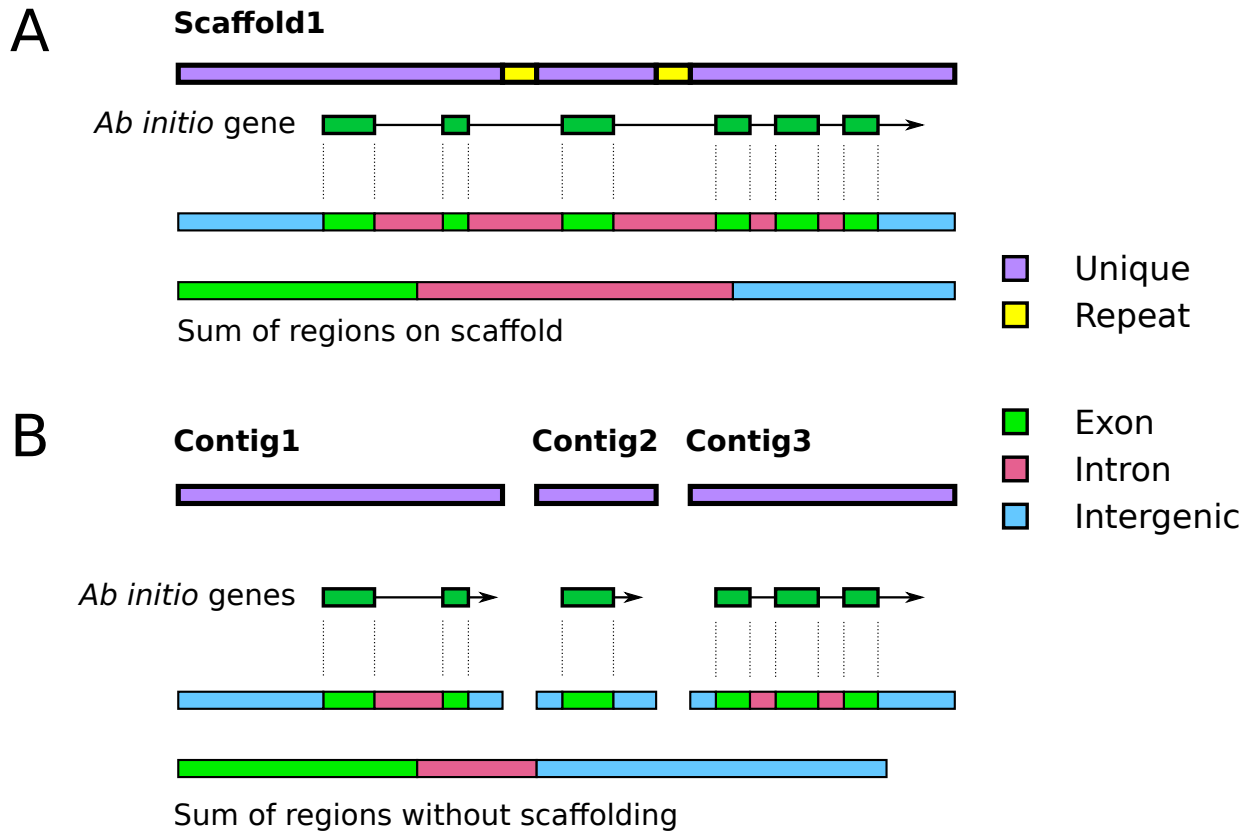


Figure 2: **Schematic of the effects of scaffolding and repeats on genic fraction analyses** (A) For a hypothetical scaffold in a genome assembly, two identical repeats are found within introns. The gene is correctly predicted to span the two repeats and the regions are defined below as in Fig 1. (B) For the case without scaffolding, or where the assembler breaks the assembly at repeats (or other high coverage regions), three contigs are generated. Note that the numbers are arbitrary, and in a real assembly they are unlikely to be in order. When annotated, all of the exons are correctly found, but the connections between them are missing for the single exon on Contig 2, resulting in a loss of intronic sequence. The final measured amount of exons is comparable, but the intron:intergenic ratio would decrease.

276 For normal diploid genomes (wild strains, not inbred lab strains), heterozygosity is not uniform across
 277 the genome. Some regions are identical between the two haplotypes (hence are homozygous alleles or loci),
 278 while others may vary by SNPs, short indels, or copy numbers of repeats, exons, or even genes. For sequences
 279 that are identical between both haplotypes, the contigs are generally kept as is, while a more complex deci-
 280 sion must be made for the heterozygous loci. During normal genome assembly, the assembler evaluates the
 281 coverage at each “bubble” (where the de Bruijn graph has two paths out of a node, and both paths merge
 282 again at the next node) and ultimately has to retain one of the paths at the exclusion of the other (Fig 3A)
 283 (also see schematics in [83] and [84]). This merging is the essential process that creates the reference genome,
 284 even though that reference is an arbitrary merge of the two haplotypes. Therefore, it must be kept in mind

285 that predicted genes or proteins in reference genomes may not be identical to either haplotype.

286

287 Regions with relatively high heterozygosity may fail to be merged in this way, leaving contigs of both
288 haplotypes in the assembly (Fig 3C). During subsequent scaffolding steps, contigs of separate haplotypes
289 can be fused head-to-tail if mate pairs are bridging the unique regions. Because this head-to-tail joining is
290 an artifact, no reads should map at the junction point, resulting in a region of zero coverage at the junction
291 and flanked by regions where coverage is half of the expected value (Fig 3D). One additional feature may
292 reveal this artifact: exons in the unmerged sections may be individually annotated but mapped ESTs or
293 *de novo* assembled transcripts may show a staggered exon pattern (Fig 3E) because transcripts can only
294 map to one of the two possible exons (2a or 2b, 3a or 3b). This may increase the ratio of intron:intergenic
295 sequence (Fig 3F), but also falsely indicate that splice variation is more prevalent for this gene.

296

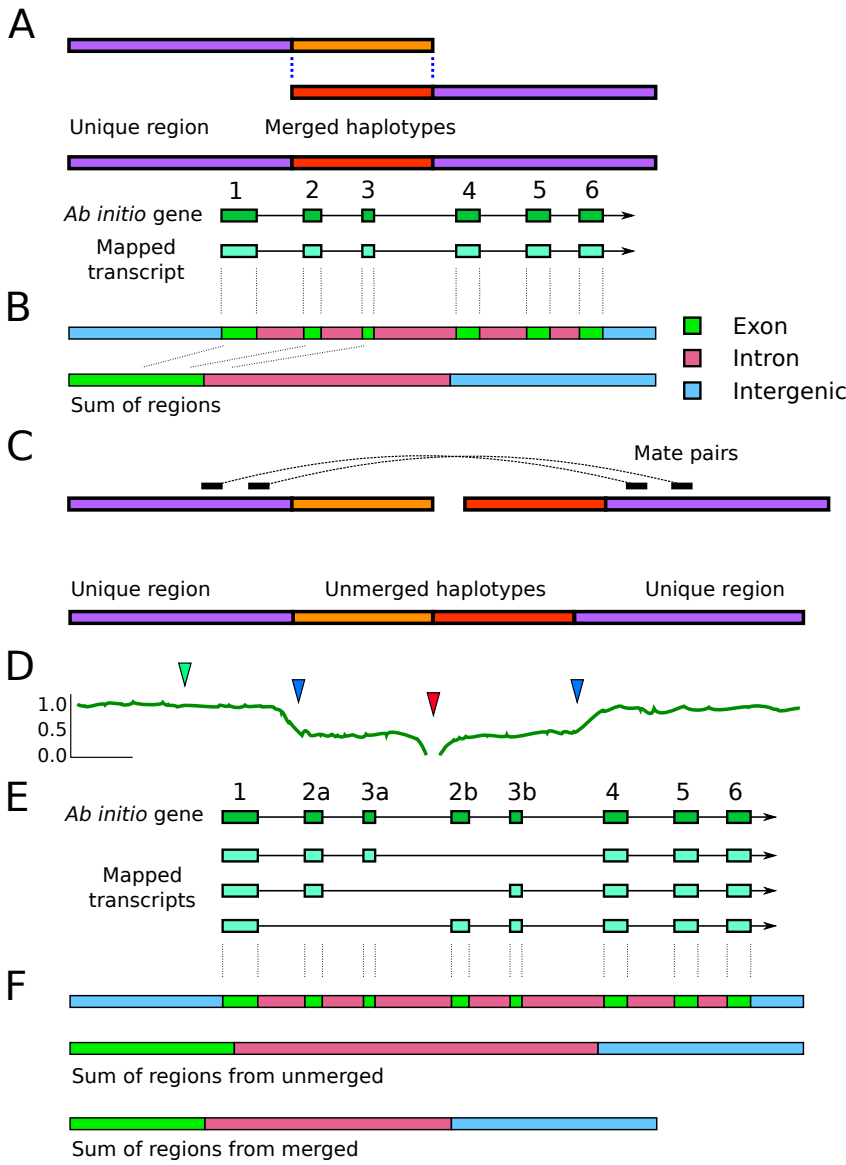


Figure 3: Schematic of misassembly and the effects on genic fraction analyses (A) During assembly, regions that are heterozygous (differing by SNPs or indels) are combined to make a single reference contig. When genes are predicting that this locus, or when assembled transcripts are aligned to the genome, the correct exon structure is found. (B) Regions are defined as exon, intron, or intergenic, as in Fig 1. (C) Reference genomes are a mix of the maternal and paternal haplotypes, but not uniformly. Rather than being merged into a single sequence, highly heterozygous regions may be assembled as different contigs that get erroneously fused during scaffolding steps. Mate pairs that bridge the two purple unique regions will instead result in a head-to-tail joining of the two unmerged haplotype sequences. (D) Hypothetical plot of read coverage across the contig. The green arrow shows a region of normal coverage (1x) while the blue arrows show sites where coverage is reduced because reads for each haplotype map separately. At the fusion point between the two haplotypes (red arrow), no reads will map since the sequence is an artifact, or is represented by a gap. (E) Mapped transcripts (or ESTs) or transcripts derived from mapped RNAseq reads (such as by Cufflinks or StringTie) may only be mapped to one of the two haplotypes, thereby producing a staggered exon structure. A mapped transcript can only align to either exon 2a or 2b, but not both, likewise for 3a or 3b, yet all other exons are unique and would align correctly. Genes predicted *ab initio* may annotate both sets of exons (2a/3a and 2b/3b), which may result in a duplication in some part of the protein, or a premature stop codon if 3a and 2b are out of phase. (F) For this hypothetical case, the sum of the regions would appear to have increased total exon size and the total intron size compared to the same genomic locus where the haplotypes were correctly merged.

297 Reannotation and changes following RNAseq reannotation

298 Keeping in mind the above error sources, some of the genomes used in our study had obvious problems of
 299 too much or too little genic content that would confound our analyses. For instance, the total amount of
 300 exons in the JGI annotation of *T. adherens* (Triad1) was only 14Mb, over twofold lower than the related
 301 species, the placozoan *H. hongkongensis*, and thus it was expected to contain many more or longer genes
 302 than were present in the original Triad1 annotation. Because of this, we remade a gene annotation for
 303 five of the species (see Methods) and used two additional publicly available annotations for *N. vectensis*
 304 and *A. queenslandica*. For most species, the reannotation dramatically increased the total amount of exons
 305 as well as the total bases of genes (Fig 4). The only exception was *B. floridae*, where the original anno-
 306 tation had predicted 90% of the genome as genes, while the reannotation had annotated only 44.8% as genes.
 307

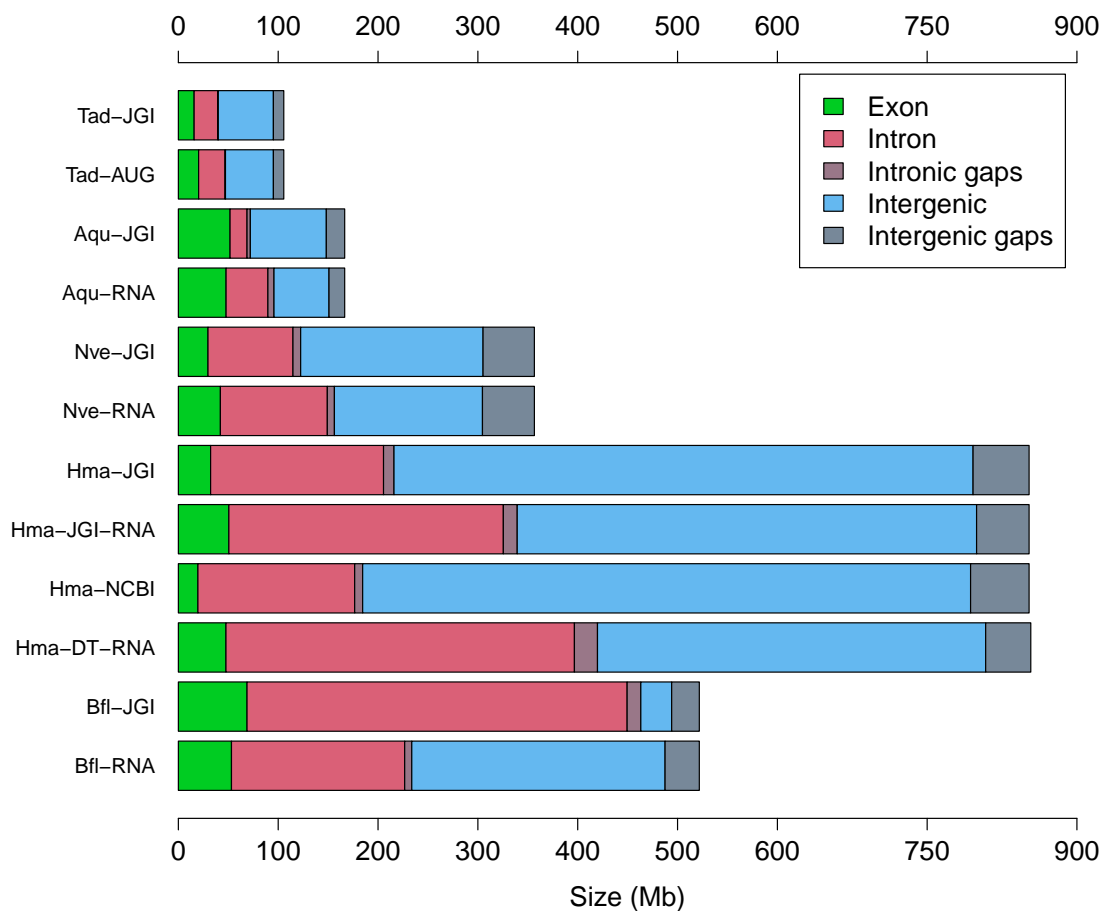


Figure 4: **Proportions of exons, introns, and intergenic sequences** Barplot showing the summed proportions of genomes composed of exons (green), introns (red) and intergenic sequences (blue). The reannotation for *O. bimaculoides* was not shown for clarity, as this genome is substantially larger than the others. Abbreviations are as follows: Tad:*T. adherens*, Aqu:*A. queenslandica*, Nve:*N. vectensis*, Hma:*H. magnipapillata*, Bfl:*B. floridae*. JGI refers to the original annotations for each species downloaded from the JGI Genome Portal. RNA refers to reannotation (see Methods) with RNAseq. Hma-NCBI is the NCBI GNOMON annotation of *H. magnipapillata*. Hma-DT-RNA is the Dovetail reassembly of *H. magnipapillata* annotated with RNAseq. AUG is the reannotation using AUGUSTUS for *T. adherens*.

308 We then compared the ratio of intron:intergenic sequence across seven of the reannotated species (Fig 5).
 309 Across these species, reannotation significantly shifted the ratio of intron:intergenic sequence, approaching a
 310 1:1 ratio (difference from 1:1 ratio, paired two-end t-test, p-value: 0.014). For *M. brevicollis*, the genome is

311 very small and the majority is exons, so the reannotation was likely to change gene boundaries (separating
 312 run-on genes) rather than defining many new genes; our reannotation contains 10,864 genes compared to
 313 the 9,196 genes in Monbr1 “best models”.
 314

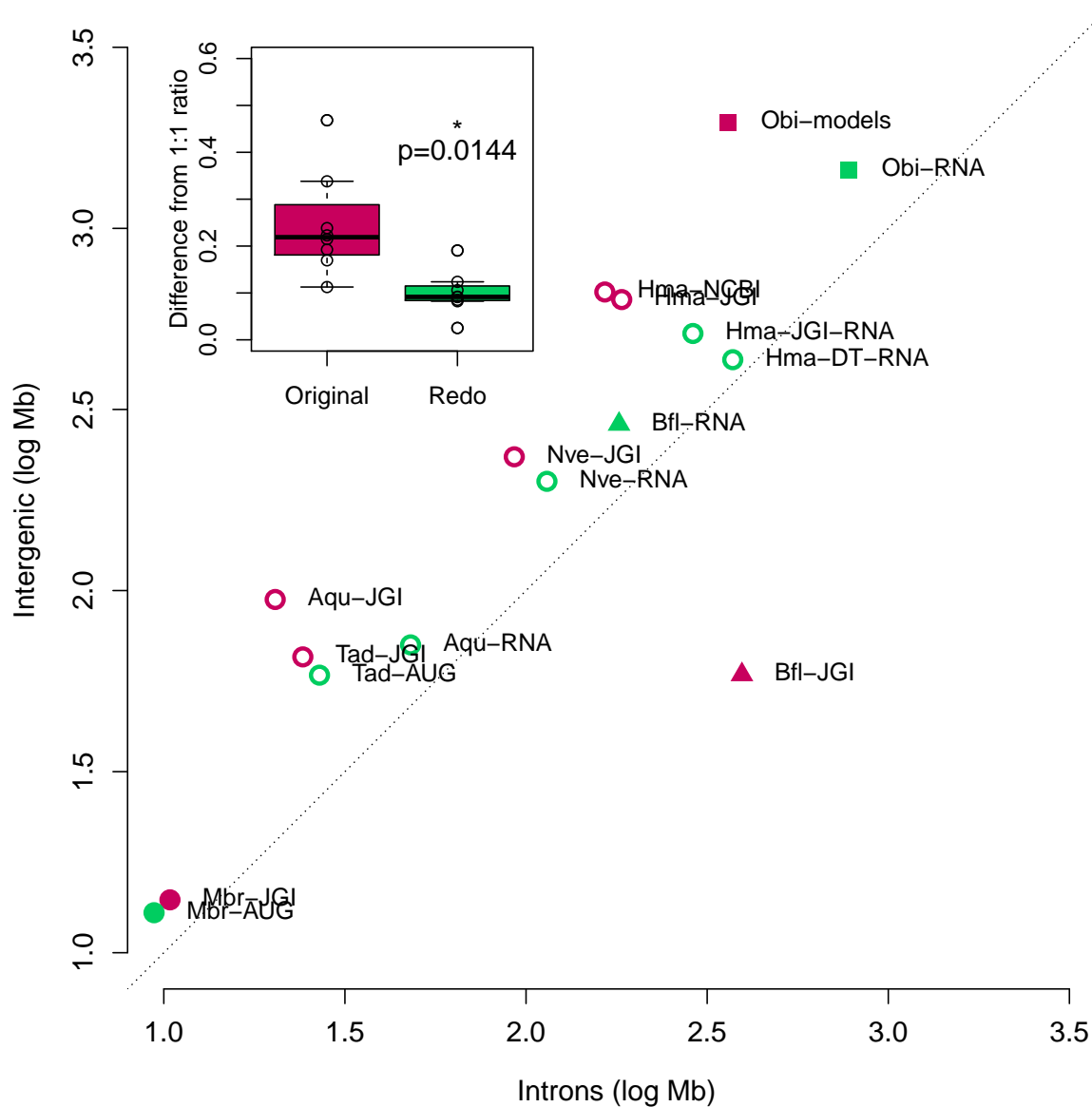


Figure 5: **Improvements from reannotation** Log-scale plot of total intronic size versus total intergenic size where original annotations from the published genomes are shown in red and reannotations are shown in green. The dotted line shows a ratio of 1:1 as a reference. Abbreviations are as in Fig 4, with the addition of Mbr: *M. brevicollis* from the original JGI annotation and the redo with AUGUSTUS, and Obi: *O. bimaculoides* from the published gene models and the reannotation with Tophat/StringTie. The inset graph shows box plot of difference of the intron:intergenic ratio to 1, showing the reannotated genomes (green) are significantly closer than the original version (paired two-end t-test, p-value: 0.0144).

315 Basic trends related to genome size

316 We observed linear correlations of total genome size to both total intronic size and intergenic size (Fig 6)
 317 (p-value: $< 10^{-37}$ for both parameters). A much weaker correlation is observed for exons (R-squared:0.3856,
 318 p-value: 10^{-8}). Because the total amount of exons in the largest genomes can be several times greater than
 319 the total size of the smallest genomes used in the study, a correlation is likely to be observed. Thus, the
 320 total amount of exons is necessarily affected by total genome size, even if this is not strongly correlated.
 321

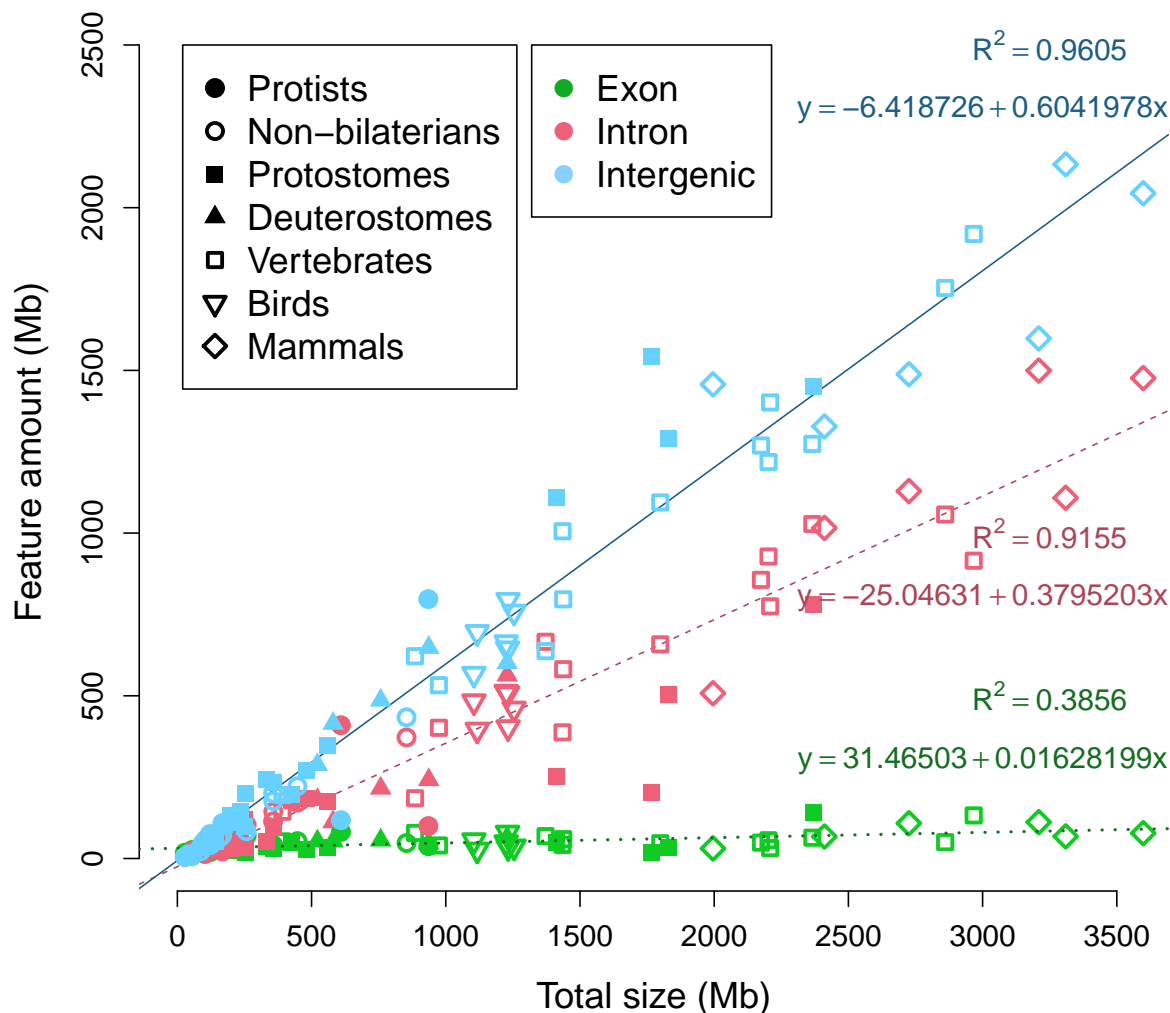


Figure 6: **Comparison of features to total genome size** The sums of exons, introns, and intergenic regions are plotted against total genome size. Linear coefficients of determination of the three features are displayed by their respective lines. For legend symbols, Deuterostomes refers to all invertebrate deuterostomes, Vertebrates excludes Birds and Mammals.

322 Average intron and exon length

323 The average length of introns linearly scales with the total genome size (Fig 7), in agreement with another
 324 study [18]. However, the average exon length is clearly constrained across animals relative to total genome
 325 size, and this may be related to interactions with nucleosomes [85]. Most species have an average exon

326 length between 200 and 300 bases (mean of 263bp), higher than values reported from previous surveys of
 327 exon length [21,86]. It must be stated that the average values presented here should not be taken as final,
 328 because variations in format of the annotations and quality of the genomes will affect the values. Since many
 329 genomes are only annotated with *ab initio* gene predictions, UTR exons may be missing from the annotation
 330 and all downstream calculations. Given that the first exon and intron tend to be longer than other exons
 331 and introns [21], respectively, absence of five-prime UTRs may result in an underestimation of the average
 332 exon length for that species.
 333

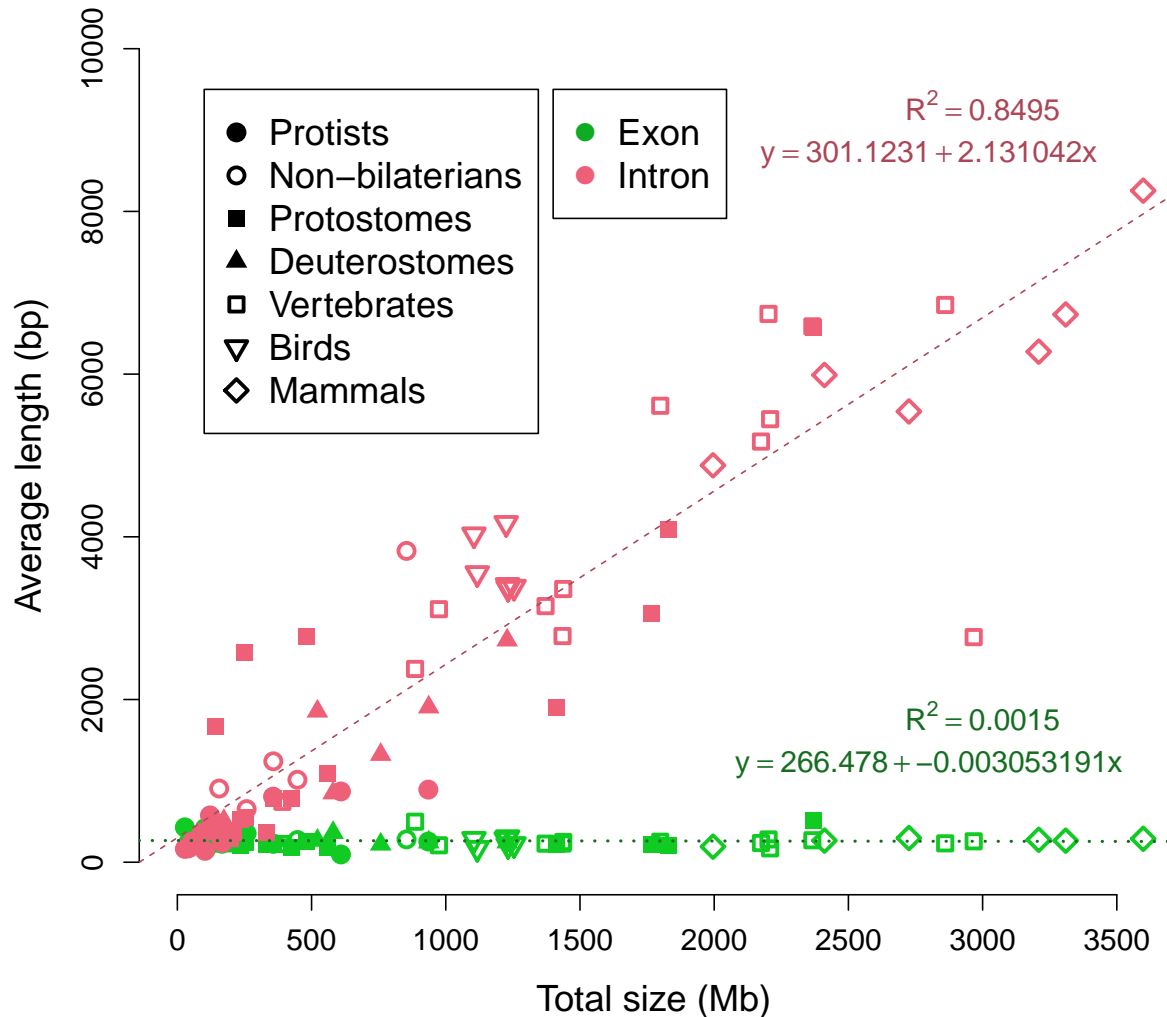


Figure 7: **Average length of exons and introns** Plot of the average length of exons (green) and introns (pink) as a function of total genome size across all species in this study. Linear coefficients of determination are displayed next to the green (dotted) and red (dashed) linear fit lines, for exons and introns, respectively.

334 Nature of the exonic fraction

335 Unlike introns or intergenic sequence, the total amount of exons does not show a strong linear correlation
 336 with total genome size (as seen in Fig 6). However, there is a hyperbolic correlation of the relative fraction of
 337 exons (megabases of exons divided by total megabases) compared to total genome size (Fig 8). The smallest
 338 genomes are dominated by exons, while the largest genomes are dominated by introns and intergenic regions.

339 This implies a relatively fixed pool of exons or coding space that becomes spread over the genome as the total
 340 size increases. The hyperbolic trend resembled the observed hyperbolic relationship between total genome
 341 size and coding proportion [18]. As coding exons are a subset of total exons, measurements of total exons
 342 may be a reasonable approximation of coding sequence, but not necessarily vice versa.
 343

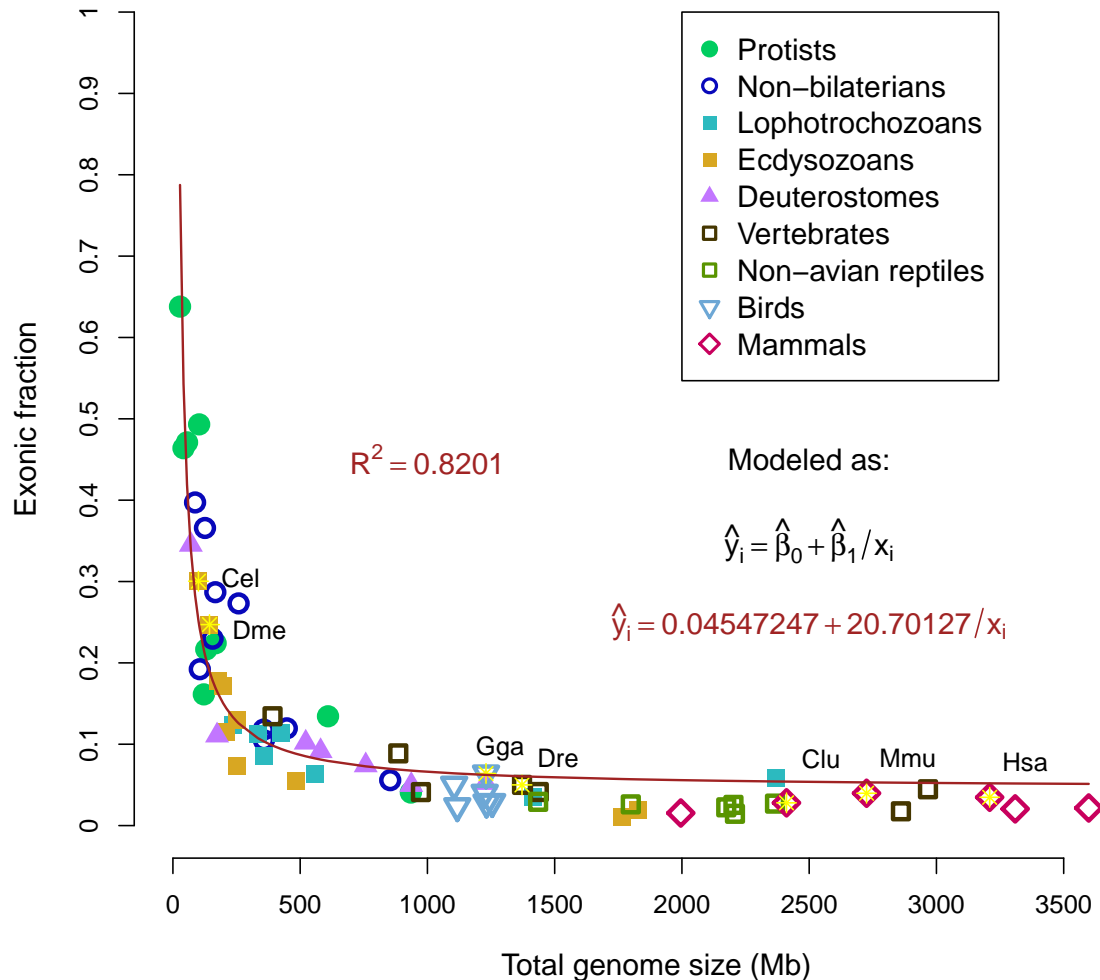


Figure 8: **Exonic fraction compared to total genome size** Relative fraction of the genome that is defined as exons compared as a function of total size. Coefficients of determination of a hyperbolic model is displayed. Seven model organisms (human, mouse, dog, chicken, zebrafish, fruit fly and nematode) are indicated by three-letter abbreviations. The formula for the fitted model is displayed in red.

344 **Ratio of introns to intergenic**

345 Because both intronic and intergenic fractions displayed a linear correlation to total genome size (Fig 6),
 346 we next examined the connection between the two fractions. While many species have a ratio of in-
 347 trons:intergenic approaching 1:1 (R-squared: 0.8286, p-value: 5.6×10^{-27}), the majority of genomes are
 348 composed of sequence annotated as intergenic regions (Fig 9).
 349

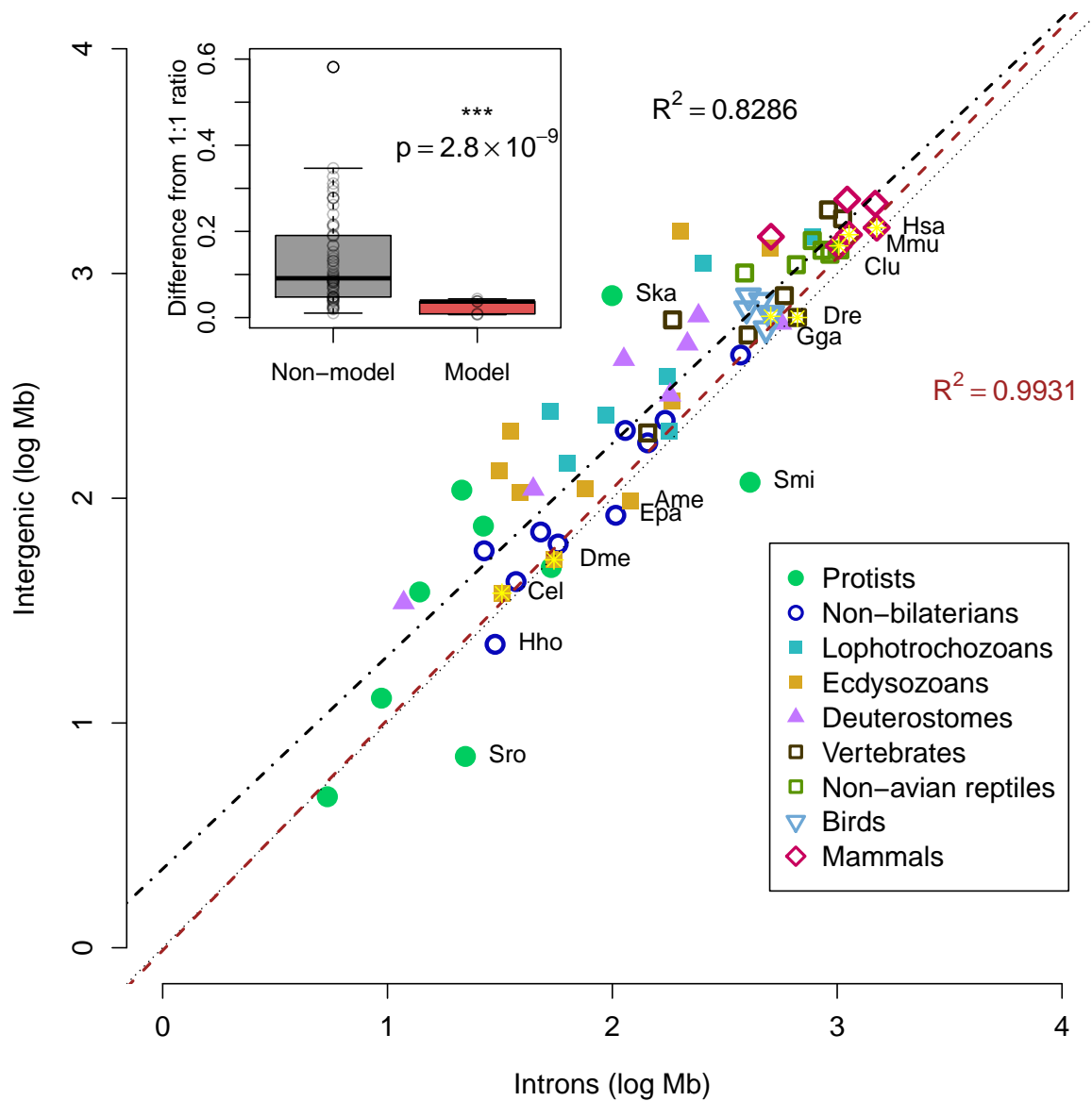


Figure 9: **Comparing intronic and intergenic fractions** Log-scale plot of total intronic size versus total intergenic size. The dotted line shows a ratio of 1:1 as a reference, although most genomes are above this line. Seven model organisms (as in Fig 8) are indicated by three-letter codes with yellow stars. Black dashed line displays the linear fit of all species in the study (R-squared: 0.8286, p-value: 5.6×10^{-27}), while the red line displays the linear fit for only the seven model organisms (R-squared: 0.9931, p-value: 1.3×10^{-6}). Names are displayed for model species, two dinoflagellates (Ska: *S. kawagutii*, Smi: *S. minutum*) and select species with ratios of intron:intergenic greater than 1, choanoflagellate *S. rosetta* (Sro), honeybee *A. mellifera* (Ame), anemone *E. pallida* (Epa), and placozoan *H. hongkongensis* (Hho). All other species names are omitted for clarity. The inset graph shows box plot of difference of the intron:intergenic ratio to 1, showing the model organisms (red) have significantly different ratios compared to the rest of the genomes (paired two-end t-test, p-value: 2.8×10^{-9}).

350 Because of the potential issue of gene annotation accuracy, we tested the linear correlation of in-
 351 trons:intergenic sequence for seven model organisms likely to have accurate annotations. A better linear

352 fit was observed when restricted to the model organisms (R-squared: 0.9931, p-value= 1.3×10^{-6}), sug-
353 gesting that deviations from the 1:1 ratio of intron:intergenic sequence are due to missing annotations,
354 rather than biological differences. Genomes of model organisms are significantly closer to the reference line
355 (two-tailed t-test, p-value: $< 10^{-7}$ for either absolute distance from 1:1 reference or absolute difference of
356 intron:intergenic ratio to 1), suggesting that the better annotations of model organisms predict a ratio of
357 1:1 of intron:intergenic sequence. Overall, the comparison of genomes of model to non-model organisms is
358 compatible with the hypothesis that the predicted amount of the genome that is transcribed varies more by
359 annotation quality than biological differences.

360
361 We then examined if there is a difference between genomes of vertebrates and invertebrates. No sig-
362 nificance difference is observed between the two model invertebrates and five vertebrates (two-tailed t-test,
363 p-value:0.99). Among all species in the study, significant differences are tenuous and highly dependent on the
364 species selected (Figure 10). For example, chordates against non-chordates is not significant (p-value:0.128)
365 while vertebrates against invertebrates is significant (p-value:0.008). However, the observed significance
366 appears to be an artifact of the abundance of low-quality genomes of protostomes, since comparison of verte-
367 brates against non-bilaterians is not significant (p-value:0.83). This difference is most simply explained by the
368 similarity between vertebrate groups. That is to say, annotation of a new mammalian genome is facilitated by
369 existing knowledge of gene structures in other mammals, rather than true differences in genome organization.

370
371 Several genomes are below the 1:1 reference line, indicating slightly more introns than intergenic, such as
372 the choanoflagellate *S. rosetta*, the honeybee *A. mellifera*, the anemone *E. pallida*, and placozoan *Hoilungia*
373 *hongkongensis*. For *A. mellifera*, it was noted that improvements in versions of the genome also included bet-
374 ter placement of repetitive intergenic sequences [71], suggesting that the relative surplus of introns is merely
375 due to the absence of some intergenic sequences in the final assembly. As for *E. pallida* and *H. hongkon-*
376 *gensis*, these species stand out as having relatively high heterozygosity, 0.4% [87] and 1.8% (manuscript
377 in preparation), respectively. Although these values are lower than the observed heterozygosity in many
378 other invertebrates [88], some highly heterozygous sequences may have caused assembly problems during
379 scaffolding (as proposed in Fig 3).

381 Evolution of the genic fraction

382 The amount of the genome that is composed of genes was highly variable across the genomes in our study,
383 ranging from 12.5% up to 87.1% of the genome. Unlike the exonic fraction, the relationship of the fraction
384 of the genome that is genes to the total size is less obvious (Fig 11), in part because this parameter is
385 most subject to gene annotation accuracy. The fraction of the genome that is exons (and perhaps coding)
386 appeared relatively fixed (Fig 8), yet the intron size was linearly correlated to the total size (Fig 6), therefore
387 the fraction that is genes (exons and introns combined) was expected to be a combination of the two trends.
388 Three correlation models were tested: hyperbolic (double-log), exponential (single-log), and linear. Of these,
389 the hyperbolic model fit best (R-square: 0.3649, p-value: $< 10^{-8}$), and no correlation was found for the other
390 models. Restricting the linear model to only genomes larger than 500Mb found essentially no correlation
391 (R-squared: 2.5×10^{-4}), suggesting that the genic fraction is unrelated to total genome size in large genomes
392 but not in small genomes.

393
394 Again, the importance of gene annotation accuracy cannot be ignored and needs to be emphasized. When
395 restricting to the seven model organisms, the range of values is narrower, from 44.9% to 62.9%. The same
396 three correlation models were applied to the genomes of model organisms, again finding that the hyperbolic
397 model best explained the variation in the genic fraction of model organisms (hyperbolic R-squared: 0.8091,
398 p-value=0.0058; exponential R-squared=0.6709; linear R-squared=0.6835). Rather than simply having no
399 correlation to total size, these results suggest that the genic fraction is fixed at around 50% in large genomes.

400

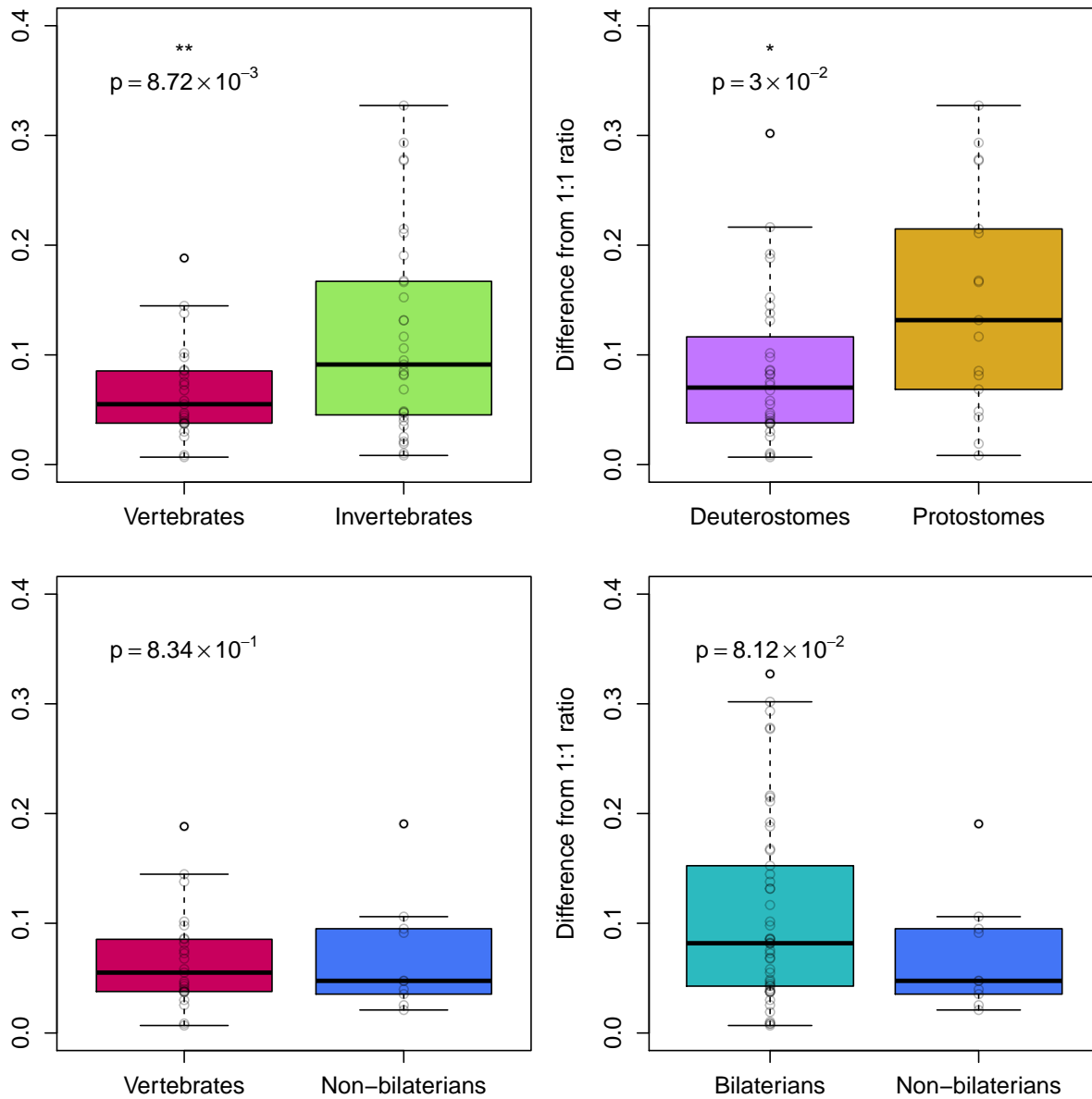


Figure 10: **Comparing intron-intergenic ratios among animal groups** Difference of the intron:intergenic ratio to 1 across four pairs of animal groups. Invertebrates (green) includes all non-bilateria taxa. Deuterostomes and protostomes are both assumed to be monophyletic.

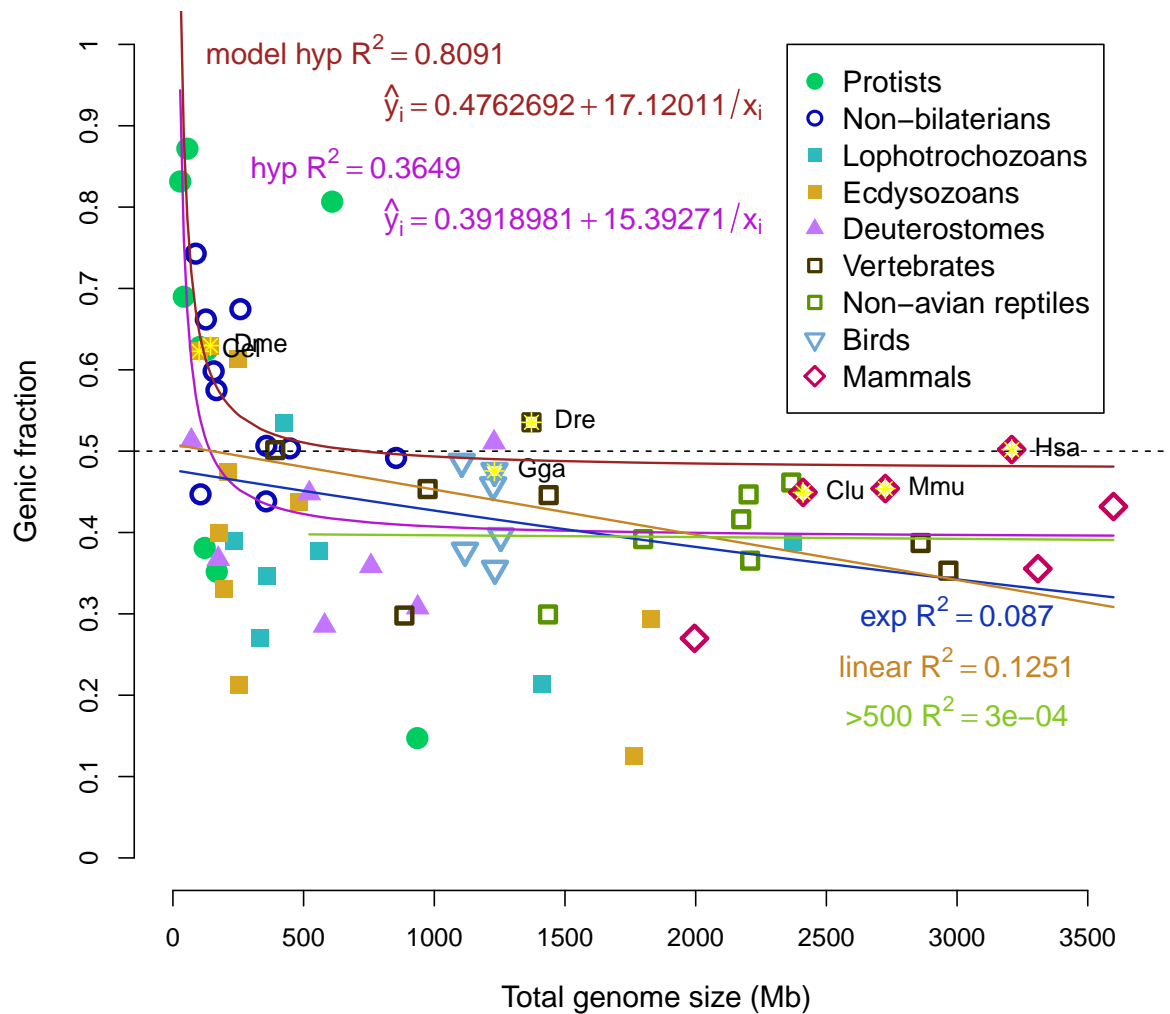


Figure 11: **Genic fraction compared to total genome size** Relative fraction of the genome that is defined as genes compared as a function of total size. A number of correlative models (hyperbolic in purple, exponential in blue, linear in orange) were tested and coefficients are displayed. Linear correlation is expected to be zero if genic and intergenic fractions “expand” indifferently after a certain size, which appears to be around 500Mb. Linear correlation including only genomes larger than 500Mb is also displayed as the green line. Seven model organisms (as in Fig 8) are indicated by three-letter codes and yellow stars. The hyperbolic correlation model for the seven model organisms is shown in red. The formulae for the fitted models are displayed in red and purple, for model organisms and all organisms, respectively.

401 Discussion

402 Diagnostic relationship of introns to intergenic sequence

403 An increasing number of genomes of any non-model organisms are sequenced to answer evolutionary ques-
404 tions. For example, genomes of taxa from all four non-bilaterian groups were recently sequenced to under-
405 stand how similar these genomes are to humans [8,24,33,34], and found that we share much more in terms of
406 genes with these groups than had been previously thought. Yet, one of the main challenges in studying the
407 genomes of non-model organisms is that there is little *a priori* information about gene structure or content.
408 It would be expected that finding orthologs of human genes is relatively easy, but does not inform us about
409 other genes that differ from humans. How should we know when we have found all of the genes? Our results
410 provide some guidance here and suggest that there is a constant ratio of introns to intergenic sequence in
411 all animals. This relationship holds even for animals with small genomes, such as the model organisms *D.*
412 *melanogaster* and *C. elegans*, suggesting that organisms with small genomes and many currently sequenced
413 invertebrates are subject to the same forces as organisms with large genomes.

415 Unusual cases of genomes

416 Based on our model, the majority of genomes appear to be underannotated, in that substantial portions of
417 the genome are not predicted to be transcribed when in fact many probably are. However, only two species,
418 the lancelet *B. floridae* and the dinoflagellate *S. minutum*, display a dramatic trend in the opposite way,
419 that is, the majority of the genome is annotated as genetic (being primarily introns).

420
421 For the lancelet *B. floridae*, the original JGI gene models had annotated almost 90% of the genome as
422 genes [23], the majority (85%) of that sequence being introns. Our reannotation of this genome displays the
423 opposite trend, where more of the genome is intergenic than intronic. The original JGI annotations did not
424 include any validation of the predicted genes, as predictions were made using mapped ESTs only as inputs
425 for the gene model training. From this, we consider it more likely that the RNAseq-based transcripts more
426 accurately resemble the true gene structures, albeit missing some genes. In addition, other evidence suggests
427 that the *B. floridae* annotations may have been unusual or erroneous [89]. A study of domain combinations
428 found that *B. floridae* had by far more fusions than any other species (across all eukaryotes) and had to be
429 excluded from the analysis [90], precisely the expected result if the majority of genes were erroneously fused.

430
431 The only other species have a much larger ratio of intron to intergenic was the dinoflagellate *S. minutum*.
432 It was described that its genome contained many long stretches of genes on the same strand, sometimes
433 continuing for hundreds of kilobases [41]. The authors also note that the *de novo* assembled transcriptome
434 appears to contain transcripts spanning multiple genes and containing multiple open reading frames, indi-
435 cating the possibility that dinoflagellate symbionts can make cistronic transcripts. This species is not an
436 animal, so it should not be assumed that animal modes of transcription are conserved across all eukaryotes.
437 However, it should be noted that a recently published genome of another symbiotic dinoflagellate species *S.*
438 *kawagutii* [40] does not display the same pattern, and instead appears to have a much greater fraction of
439 intergenic regions than introns.

441 Genome composition across metazoa

442 Previous studies have discussed problems with trying to relate the number of genes to the size of the
443 genome [91–93]. One study [18] found a weak positive correlation between genome size and number of
444 genes. This parallels our finding that total exonic sequence is weakly correlated to total genome size (Fig 6).
445 However, this measurement can be problematic if the genome assembly is highly fragmented, containing a
446 large number of short contigs or scaffolds. In such cases, gene number is unlikely to correlate to genome
447 size for the same reason as the difficulties in predicting the genic fraction, that is, it is strongly affected by
448 gene annotation errors. In our schematic (Fig 2), a gene that is split up onto three contigs would therefore
449 be counted as three genes, albeit short ones. If this occurs on a genome-wide scale, the count of genes will

450 be inaccurate. Parts of genes would be individually annotated as genes, increasing the total gene number
451 without much change to the total number of exonic bases.

452
453 Rather than relying on counts of genes or determining coding sequence, we instead examined sequence
454 that is annotated as exons. We found that while a weak positive correlation is observed between total exonic
455 bases and genome size, most of the difference in size is related to introns and intergenic sequence. The
456 amount of the genome that is composed of introns is linearly related to the total genome size (Fig 6). Also
457 considering the measured linear correlation of intergenic sequence to total size, it is not surprising that most
458 species have roughly a 1:1 ratio of introns:intergenic sequence (Fig 9). This appears to be the case regardless
459 of genome size or the total exonic sequence. For instance, the genome of the choanoflagellate *M. brevicollis*
460 has 9.3Mb of introns and 10.1Mb of intergenic sequence (a ratio of 0.92) compared to 19.3Mb of exons.

461
462 Therefore, model animals (and probably all animals) transcribe nearly half of the genome, where species
463 with smaller genomes (exon-rich) transcribe more than half (Figure 11). There does not appear to be a
464 significant difference in the genic fraction based on animal group (Figure 10), that is, all animals appear to
465 follow this rule. One study had shown that some larger metazoan genomes were depleted in genes [94], yet
466 this study made use of a small number of species for comparison and included several chordates known for
467 their very small genomes, the tunicate *C. intestinalis* and the pufferfish *T. rubripes*. The authors examined
468 windows of 50kb and found that 80% of the human genome was lacking any gene [94], though it is unclear
469 if this analysis was restricted to protein coding genes. However, we found that 50.2% of the human genome
470 is composed of genes (93% of that is introns).

471
472 While genomes of the model organisms and many non-models organisms appear to follow the hyperbolic
473 relationship of genic fraction to size, nonetheless, a large number of the genomes in this study appear to be
474 composed of much less than 50% genes. That observation is best explained by the hypothesis that many
475 genomes are missing genes. These missing genes may or may not be coding, though perhaps missing gene
476 content is made of lineage-specific proteins. Because annotation of the genome by RNAseq per se cannot
477 distinguish coding genes from non-coding ones, we could not determine coding fractions for all species. Even
478 for putative non-coding transcripts, some may be coding [95–97], thus protein sequencing may reveal the
479 true nature of these transcripts.

481 Evolution of genomes

482 The genic fraction has a hyperbolic relationship to the total genome size. The modeled curve flattens around
483 500Mb, after that point, introns and intergenic regions are expected to expand, on average, equally across
484 the genome resulting in approximately 50% of the genome as genes (the majority of that being introns) and
485 the other 50% as intergenic sequence. It should be noted that larger genomes still have more exonic bases
486 than small genomes, though the difference in total genome size across animals is mostly from introns or
487 intergenic sequence.

488
489 It has been theorized that changes in genome size are a balance between short deletions and long in-
490 sertions [98]. If the last common ancestor of all metazoans had a relatively small genome (under 100Mb,
491 resembling some single-cell eukaryotes in our study), then the majority of modern animals have undergone
492 dramatic expansion of their genomes, meaning dominated by insertions or duplications. How does this ex-
493 pansion occur and does it favor a novel origin of introns or expansion of intergenic sequences? Following
494 the trend in Fig 9 and Fig 11, it appears that small genomes are dominated by genes because they are
495 mostly exons, and both genes and intergenic sequences are expanded in equally as the genomes enlarge.
496 Mechanistically, these insertions are likely to be mediated by transposable elements or replication errors. As
497 small genomes become invaded by transposable elements (perhaps following some genomic stress like genome
498 duplication), introns appear and expand at roughly the same rate as intergenic sequences producing a 1:1
499 ratio of intron:intergenic across all species (Fig 9).

500
501 Above a certain size (around 500Mb), genic and intergenic sequences expand almost equally, where 50%

502 of the genome is genic; exons comprise an almost negligible fraction of the genome, which is otherwise
503 composed of approximately equal fractions of introns and intergenic sequences. This might be explained by
504 changes in diversity of transposable elements, as the highest diversity was found in genomes ranging from
505 500Mb to 1.5Gb [17]. Larger genomes appeared to be flooded by transposable elements of a single type.
506 Thus, above 500Mb, it can be predicted that select transposable elements become prevalent and multiply
507 throughout the genome, but on average end up expanding introns and intergenic sequences equally.

508

509 Relationship to phenotypic complexity

510 The size of the genome can vary greatly even for closely related organisms. This has been called the “c-value
511 paradox” [1,99], based on the observation that although the many organisms have larger genomes relative to
512 similar species (bigger “c-value”), this measurement does not equate with more or less complex organisms in
513 a straightforward way. A classic example of this is frog genus *Xenopus*, where the genome of the species *X.*
514 *laevis* is almost twice as large as the species *X. tropicalis* [100], though the animal is not twice as “complex”.
515 Similar observations have been made that the number of genes appears unrelated to the size of the genome
516 and the complexity (sometimes called the “g-value paradox” [91,101]).

517

518 If neither genome size nor gene number are clearly related to complexity, then what is? Another relation-
519 ship has been proposed between the usage of alternative splice variants and organismic complexity because
520 variation in splicing can increase the number of potential proteins from an overall fixed pool of exons [102].
521 Vertebrates and specifically mammals tend to splice transcripts more than invertebrates (meaning models
522 fruit fly and nematode) [103,104]. One study reported a good correlation (R-squared of 0.80) of splicing to
523 organismic complexity measured by cell types [105], but also reported that this trend effectively disappeared
524 when correcting for sequencing depth, using the number of ESTs available as a proxy for annotation quality.
525 The largest invertebrate genome used in that study was the deer tick *I. scapularis*, which did have a mea-
526 sured number of cell types but unfortunately could not be analyzed further, leaving the bulk of the analysis
527 weighted heavily by mammals and small-genome insects.

528

529 However, other studies report that alternative splicing is more frequent when the surrounding introns
530 are long [106,107], suggesting that organisms with large genomes (and therefore larger introns) might be
531 predisposed to splice. This could suggest that some of the invertebrates in our study may have more complex
532 splicing patterns than are annotated in the current genome versions. For the largest invertebrate genome in
533 our study, the octopus *O. bimaculoides*, only 14.8% of loci appeared to have alternative splice variants [45].
534 In our reannotation we found only 6.4% of all loci have any type of splice variant. However, the majority
535 of predicted transcripts (75%) are single exon loci, and possibly many genes are fragmented across multiple
536 contigs (as in Figure 2). When restricted to loci with multiple exons (15% of total loci), 41% have more than
537 one variant. These data from *O. bimaculoides* suggested that overall patterns in splicing do not display a
538 reliable connection to organismic complexity when complexity is generalized across animal groups. However,
539 without proper measurements of cell types from the octopus, it cannot be assumed that the number of cell
540 types resembles the value for the fruit fly, which was implicit in other studies given that all protostomes were
541 effectively represented by insects [105]. Thus, it could be the case that the octopus, with a large genome,
542 has a large number of cell types and many genes are spliced, all in agreement with the splicing-complexity
543 hypothesis.

544

545 It is a challenge to separate these observations from biases in sequencing depth (of transcripts or ESTs)
546 and data availability. In our study, we could only make use of five invertebrates with relatively large genomes,
547 the cnidarian *H. magnipapillata*, the pearl oyster *P. fucata*, the horseshoe crab *L. polyphemus*, the deer tick
548 *I. scapularis*, and the octopus *O. bimaculoides*. On the other hand, NCBI has over 100 genomes of mammals
549 available for download. Alternatively, the repertoire of splice factors or the genes that are most spliced may
550 be of greater importance than just splicing in general. Our understanding is likely to be improved with more
551 deeply-sequenced transcriptomes from large-genome invertebrates.

552

553 Limitations

554 Because we were making use of mostly public data, our analyses were subject to both technical and biological
555 limitations. There are a small number of taxa with sequenced genomes from many invertebrate groups.
556 Because the majority of sequenced vertebrate genomes are large and the majority of sequenced invertebrate
557 genomes are small [92], the axis of simple invertebrate to complex vertebrate is synonymous with small to
558 large genomes, and thus the prevalence of splicing in large-genome animals may be a consequence of the size
559 of the genome and complexity may be only correlated. This issue is not simple to resolve, as there may not
560 be members in all animal groups with both small and large genomes. For instance, a survey of genome sizes
561 across Porifera stated that the largest genome out of the 70 species sampled was around 600Mb [108]. Thus,
562 there may not be any “large” genomes in this phylum, and likewise for other invertebrate groups. Compared
563 to birds, however, where the smallest genome identified to date is from the black-chinned hummingbird
564 (estimated 910Mb) [109], perhaps no bird will be found that has a “small” genome.

565
566 Our use of public genome annotations was limited in part from difficulties in defining elements. Much like
567 definitions of transcribed pseudogenes, the identification of long-intergenic non-coding RNAs, or lincRNAs,
568 presents a paradox of definitions. Non-coding RNAs with known functions are arguably genes, such as the
569 X-inactivation transcript Xist, thus any functional transcribed intergenic RNA is by definition not intergenic;
570 it is genic. This distinction rests upon discovery of a function of these putative RNAs. In the context of
571 the ENCODE project or MouseENCODE [110], transcription was found of intergenic regions accounting
572 for almost another 20% of the genomes of human and mouse, depending on the analysis [111, 112]. If this
573 were all functional, then the genic fraction of the genome would be far above 50% for large genomes and
574 the ratio of intron:intergenic sequence would not be expected to be close to 1:1. Alternatively, if most of
575 these intergenic transcripts are non-functional “noise”, then our results are supported as presented. There-
576 fore, consideration of the importance or genic quality rests upon the distinction between functional RNAs
577 and noisy transcription. Existing data are not adequate to identify functions, but several experiments may
578 improve our understanding. Conceptually, the most straightforward approach is knocking out regions of
579 transcribed “gene deserts” in mouse or human cells, but on a larger scale than a previous study [113]. Ad-
580 ditionally, better models of transcriptional noise or random transcription may inform whether or not the
581 observed transcriptional patterns from the ENCODE project are consistent with noise.

583 Conclusion

584 We have shown that a set of animals from 12 phyla transcribe at least half of their genomes in a size-
585 dependent fashion. For large genomes, the amount of exons is almost negligible, where introns account for
586 most of the genic sequence. In such cases, genic sequence is almost equal to the amount of intergenic sequence.
587 Whereas for small genomes, exons can be a major fraction of the genome, resulting in the appearance of
588 gene-dense genomes. This parity between introns and intergenic sequence is likely a universal feature of
589 animal genomes, though this may be tested with addition of many more animal taxa from other phyla that
590 do not have sequenced members. Previous findings of genomic differences between animal groups are likely
591 to result from a sampling bias, rather than biological differences. Future improvements in assembly and
592 annotation of animal genomes may reveal unanticipated sources of complexity and gene regulation with
593 implications for the evolution of animals.

594 Acknowledgments

595 W.R.F would like to thank M. Eitel for helpful comments on the manuscript. This work was supported by a
596 LMUexcellent grant (Project MODELSPONGE) to G.W. as part of the German Excellence Initiative. The
597 authors declare no competing interests.

References

- 598
- 599 [1] Thomas CA. The Genetic Organization of Chromosomes. *Annual review of genetics*. 1971;5(1):237–
600 256. doi:10.1146/annurev.ge.05.120171.001321.
- 601 [2] Han K, Li Zf, Peng R, Zhu Lp, Zhou T, Wang Lg, et al. Extraordinary expansion of a *Sorangium*
602 *cellulosum* genome from an alkaline milieu. *Scientific reports*. 2013;3:2101. doi:10.1038/srep02101.
- 603 [3] Brent MR. Steady progress and recent breakthroughs in the accuracy of automated genome annotation.
604 *Nature reviews Genetics*. 2008;9(1):62–73. doi:10.1038/nrg2220.
- 605 [4] Guigó R, Flicek P, Abril JF, Reymond A, Lagarde J, Denoeud F, et al. EGASP: the human EN-
606 CODE Genome Annotation Assessment Project. *Genome biology*. 2006;7 Suppl 1(Suppl 1):S2.1–31.
607 doi:10.1186/gb-2006-7-s1-s2.
- 608 [5] Vallender EJ. Bioinformatic approaches to identifying orthologs and assessing evolutionary relation-
609 ships. *Methods*. 2009;49(1):50–55. doi:10.1016/j.ymeth.2009.05.010.
- 610 [6] Zhang X, Goodsell J, Norgren RB. Limitations of the rhesus macaque draft genome assembly and
611 annotation. *BMC genomics*. 2012;13(1):206. doi:10.1186/1471-2164-13-206.
- 612 [7] Altenhoff AM, Boeckmann B, Capella-Gutierrez S, Dalquen DA, DeLuca T, Forslund K, et al.
613 Standardized benchmarking in the quest for orthologs. *Nature Methods*. 2016;13(5):425–430.
614 doi:10.1038/nmeth.3830.
- 615 [8] Ryan JF, Pang K, Schnitzler CE, a D Nguyen Ad, Moreland RT, Simmons DK, et al. The
616 Genome of the Ctenophore *Mnemiopsis leidyi* and Its Implications for Cell Type Evolution. *Science*.
617 2013;342(6164):1242592–1242592. doi:10.1126/science.1242592.
- 618 [9] Pisani D, Pett W, Dohrmann M, Feuda R, Rota-Stabelli O, Philippe H, et al. Genomic data do not
619 support comb jellies as the sister group to all other animals. *Proceedings of the National Academy of*
620 *Sciences*. 2015;112(50):201518127. doi:10.1073/pnas.1518127112.
- 621 [10] Parra G, Bradnam K, Korf I. CEGMA: a pipeline to accurately annotate core genes in eukaryotic
622 genomes. *Bioinformatics (Oxford, England)*. 2007;23(9):1061–7. doi:10.1093/bioinformatics/btm071.
- 623 [11] Simão FA, Waterhouse RM, Ioannidis P, Kriventseva EV. BUSCO : assessing genome assem-
624 bly and annotation completeness with single-copy orthologs. *Genome analysis*. 2015;31(June):9–10.
625 doi:10.1093/bioinformatics/btv351.
- 626 [12] Lynch M, Conery JS. The origins of genome complexity. *Science (New York, NY)*. 2003;302(5649):1401–
627 4. doi:10.1126/science.1089370.
- 628 [13] Lynch M. Response to Comment on "The Origins of Genome Complexity". *Science*.
629 2004;306(5698):978b–978b. doi:10.1126/science.1100559.
- 630 [14] Daubin V, Moran Na. Comment on "The origins of genome complexity". *Science (New York, NY)*.
631 2004;306(5698):978; author reply 978. doi:10.1126/science.1098469.
- 632 [15] Pettersson ME, Kurland CG, Berg OG. Deletion rate evolution and its effect on genome size and
633 coding density. *Molecular Biology and Evolution*. 2009;26(6):1421–1430. doi:10.1093/molbev/msp054.
- 634 [16] Kidwell MG. Transposable elements and the evolution of genome size in eukaryotes. *Genetica*.
635 2002;115(1):49–63. doi:10.1023/A:1016072014259.
- 636 [17] Elliott TA, Gregory TR. Do larger genomes contain more diverse transposable elements? *BMC*
637 *evolutionary biology*. 2015;15(1):69. doi:10.1186/s12862-015-0339-8.
- 638 [18] Elliott TA, Gregory TR. What's in a genome? The C-value enigma and the evolution of eukaryotic
639 genome content. *Phil Trans R Soc B*. 2015;370(1678):20140331. doi:10.1098/rstb.2014.0331.

- 640 [19] Canapa A, Barucca M, Biscotti MA, Forconi M, Olmo E. Transposons, Genome Size, and Evolutionary
641 Insights in Animals. *Cytogenetic and Genome Research*. 2016; p. 217–239. doi:10.1159/000444429.
- 642 [20] Deutsch M, Long M. Intron-exon structures of eukaryotic model organisms. *Nucleic acids research*.
643 1999;27(15):3219–28.
- 644 [21] Zhu L, Zhang Y, Zhang W, Yang S, Chen JQ, Tian D. Patterns of exon-intron architecture variation
645 of genes in eukaryotic genomes. *BMC genomics*. 2009;10(1):47. doi:10.1186/1471-2164-10-47.
- 646 [22] Dehal P, Satou Y, Campbell RK, Chapman J, Degnan B, De Tomaso A, et al. The draft genome
647 of *Ciona intestinalis*: insights into chordate and vertebrate origins. *Science (New York, NY)*.
648 2002;298(5601):2157–2167. doi:10.1126/science.1080049.
- 649 [23] Putnam NH, Butts T, Ferrier DEK, Furlong RF, Hellsten U, Kawashima T, et al. The am-
650 phioxus genome and the evolution of the chordate karyotype. *Nature*. 2008;453(7198):1064–71.
651 doi:10.1038/nature06967.
- 652 [24] Srivastava M, Begovic E, Chapman J, Putnam NH, Hellsten U, Kawashima T, et al. The Trichoplax
653 genome and the nature of placozoans. *Nature*. 2008;454(7207):955–60. doi:10.1038/nature07191.
- 654 [25] Simakov O, Marletaz F, Cho SJ, Edsinger-Gonzales E, Havlak P, Hellsten U, et al. Insights into bilate-
655 rian evolution from three spiralian genomes. *Nature*. 2013;493(7433):526–31. doi:10.1038/nature11696.
- 656 [26] Simakov O, Kawashima T, Marlétaz F, Jenkins J, Koyanagi R, Mitros T, et al. Hemichordate genomes
657 and deuterostome origins. *Nature*. 2015; p. 1–19. doi:10.1038/nature16150.
- 658 [27] King N, Westbrook MJ, Young SL, Kuo A, Abedin M, Chapman J, et al. The genome of the
659 choanoflagellate *Monosiga brevicollis* and the origin of metazoans. *Nature*. 2008;451(7180):783–8.
660 doi:10.1038/nature06617.
- 661 [28] Read Ba, Kegel J, Klute MJ, Kuo A, Lefebvre SC, Maumus F, et al. Pan genome of the phytoplankton
662 *Emiliania underpins* its global distribution. *Nature*. 2013; p. 9–13. doi:10.1038/nature12221.
- 663 [29] Prochnik SE, Umen J, Nedelcu AM, Hallmann A, Miller SM, Nishii I, et al. Genomic analysis
664 of organismal complexity in the multicellular green alga *Volvox carteri*. *Science (New York, NY)*.
665 2010;329(5988):223–6. doi:10.1126/science.1188800.
- 666 [30] Suga H, Chen Z, de Mendoza A, Sebé-Pedrós A, Brown MW, Kramer E, et al. The *Capsaspora*
667 genome reveals a complex unicellular prehistory of animals. *Nature communications*. 2013;4:2325.
668 doi:10.1038/ncomms3325.
- 669 [31] Fairclough SR, Chen Z, Kramer E, Zeng Q, Young S, Robertson HM, et al. Premetazoan genome
670 evolution and the regulation of cell differentiation in the choanoflagellate *Salpingoeca rosetta*. *Genome*
671 *biology*. 2013;14(2):R15. doi:10.1186/gb-2013-14-2-r15.
- 672 [32] Fernandez-Valverde SL, Calcino AD, Degnan BM. Deep developmental transcriptome sequencing
673 uncovers numerous new genes and enhances gene annotation in the sponge *Amphimedon queenslandica*.
674 *BMC Genomics*. 2015;16(1):1–11. doi:10.1186/s12864-015-1588-z.
- 675 [33] Srivastava M, Simakov O, Chapman J, Fahey B, Gauthier MEa, Mitros T, et al. The *Amphime-*
676 *don queenslandica* genome and the evolution of animal complexity. *Nature*. 2010;466(7307):720–6.
677 doi:10.1038/nature09201.
- 678 [34] Putnam NH, Srivastava M, Hellsten U, Dirks B, Chapman J, Salamov A, et al. Sea anemone genome
679 reveals ancestral eumetazoan gene repertoire and genomic organization. *Science (New York, NY)*.
680 2007;317(5834):86–94. doi:10.1126/science.1139158.
- 681 [35] Moran Y, Fredman D, Praher D, Li XZ, Wee LM, Rentzsch F, et al. Cnidarian microRNAs frequently
682 regulate targets by cleavage. *Genome Research*. 2014;24(4):651–663. doi:10.1101/gr.162503.113.

- 683 [36] Fortunato SaV, Adamski M, Ramos OM, Leininger S, Liu J, Ferrier DEK, et al. Calcisponges have a
684 ParaHox gene and dynamic expression of dispersed NK homeobox genes. *Nature*. 2014;514(7524):620–
685 623. doi:10.1038/nature13881.
- 686 [37] Voskoboynik A, Neff NF, Sahoo D, Newman AM, Pushkarev D, Koh W, et al. The genome sequence
687 of the colonial chordate, *Botryllus schlosseri*. *eLife*. 2013;2:e00569. doi:10.7554/eLife.00569.
- 688 [38] Baumgarten S, Simakov O, Esherrick LY, Liew YJ, Lehnert EM, Michell CT, et al. The genome of
689 *Aiptasia*, a sea anemone model for coral symbiosis. *Proceedings of the National Academy of Sciences*.
690 2015; p. 201513318. doi:10.1073/pnas.1513318112.
- 691 [39] Deroeud F, Henriot S, Mungpakdee S, Aury JM, Da Silva C, Brinkmann H, et al. Plasticity of Animal
692 Genome Architecture Unmasked by Rapid Evolution of a Pelagic Tunicate. *Science*. 2010;1381(2010).
693 doi:10.1126/science.1194167.
- 694 [40] Lin S, Cheng S, Song B, Zhong X, Lin X, Li W, et al. The *Symbiodinium kawagutii* genome
695 illuminates dinoflagellate gene expression and coral symbiosis. *Science*. 2015;350(6261):691–694.
696 doi:10.1126/science.aad0408.
- 697 [41] Shoguchi E, Shinzato C, Kawashima T, Gyoja F, Mungpakdee S, Koyanagi R, et al. Draft Assembly of
698 the *Symbiodinium minutum* Nuclear Genome Reveals Dinoflagellate Gene Structure. *Current biology*
699 : CB. 2013;23:1399–1408. doi:10.1016/j.cub.2013.05.062.
- 700 [42] Takeuchi T, Kawashima T, Koyanagi R, Gyoja F, Tanaka M, Ikuta T, et al. Draft genome of
701 the pearl oyster *Pinctada fucata*: a platform for understanding bivalve biology. *DNA research* :
702 an international journal for rapid publication of reports on genes and genomes. 2012;19(2):117–30.
703 doi:10.1093/dnares/dss005.
- 704 [43] Shinzato C, Shoguchi E, Kawashima T, Hamada M, Hisata K, Tanaka M, et al. Using the *Acropora*
705 *digitifera* genome to understand coral responses to environmental change. *Nature*. 2011;476(7360):320–
706 3. doi:10.1038/nature10249.
- 707 [44] Luo YJ, Takeuchi T, Koyanagi R, Yamada L, Kanda M, Khalturina M, et al. The *Lingula* genome
708 provides insights into brachiopod evolution and the origin of phosphate biomineralization. *Nature*
709 *Communications*. 2015;6:1–10. doi:10.1038/ncomms9301.
- 710 [45] Albertin CB, Simakov O, Mitros T, Wang ZY, Pungor JR, Edsinger-gonzales E, et al. The
711 octopus genome and the evolution of cephalopod neural and morphological novelties. *Nature*.
712 2015;doi:10.1038/nature14668.
- 713 [46] Kirkness EF. The Dog Genome: Survey Sequencing and Comparative Analysis. *Science*.
714 2003;301(5641):1898–1903. doi:10.1126/science.1086432.
- 715 [47] Mikkelsen TS, Wakefield MJ, Aken B, Amemiya CT, Chang JL, Duke S, et al. Genome of the marsupial
716 *Monodelphis domestica* reveals innovation in non-coding sequences. *Nature*. 2007;447(7141):167–77.
717 doi:10.1038/nature05805.
- 718 [48] Warren WC, Hillier LW, Marshall Graves JA, Birney E, Ponting CP, Grützner F, et al. Genome
719 analysis of the platypus reveals unique signatures of evolution. *Nature*. 2008;453(7192):175–183.
720 doi:10.1038/nature06936.
- 721 [49] Hellsten U, Harland RM, Gilchrist MJ, Hendrix D, Jurka J, Kapitonov V, et al. The genome
722 of the Western clawed frog *Xenopus tropicalis*. *Science (New York, NY)*. 2010;328(5978):633–6.
723 doi:10.1126/science.1183670.
- 724 [50] Zhang G, Li C, Li Q, Li B, Larkin DM, Lee C, et al. Comparative genomics reveals insights into avian
725 genome evolution and adaptation. *Science*. 2014;346(6215):1311–1320. doi:10.1126/science.1251385.
- 726 [51] Warren WC, Clayton DF, Ellegren H, Arnold AP, Hillier LW, Künstner A, et al. The genome of a
727 songbird. *Nature*. 2010;464(7289):757–62. doi:10.1038/nature08819.

- 728 [52] Huang Y, Li Y, Burt DW, Chen H, Zhang Y, Qian W, et al. The duck genome and transcriptome
729 provide insight into an avian influenza virus reservoir species. *Nature genetics*. 2013;45(7):776–83.
730 doi:10.1038/ng.2657.
- 731 [53] Ganapathy G, Howard JT, Ward JM, Li J, Li B, Li Y, et al. High-coverage sequencing and annotated
732 assemblies of the budgerigar genome. *GigaScience*. 2014;3:11. doi:10.1186/2047-217X-3-11.
- 733 [54] Green RE, Braun EL, Armstrong J, Earl D, Nguyen N, Hickey G, et al. Three crocodylian genomes
734 reveal ancestral patterns of evolution among archosaurs. *Science*. 2014;346(6215):1254449–1254449.
735 doi:10.1126/science.1254449.
- 736 [55] Alföldi J, Di Palma F, Grabherr M, Williams C, Kong L, Mauceli E, et al. The genome of the green
737 anole lizard and a comparative analysis with birds and mammals. *Nature*. 2011;477(7366):587–91.
738 doi:10.1038/nature10390.
- 739 [56] Shaffer HB, Minx P, Warren DE, Shedlock AM, Thomson RC, Valenzuela N, et al. The western
740 painted turtle genome, a model for the evolution of extreme physiological adaptations in a slowly
741 evolving lineage. *Genome biology*. 2013;14(3):R28. doi:10.1186/gb-2013-14-3-r28.
- 742 [57] Wang Z, Pascual-Anaya J, Zadissa A, Li W, Niimura Y, Huang Z, et al. The draft genomes of soft-shell
743 turtle and green sea turtle yield insights into the development and evolution of the turtle-specific body
744 plan. *Nature Genetics*. 2013;45(6):701–706. doi:10.1038/ng.2615.
- 745 [58] Koning APJD, Hall KT, Card DC, Drew R, Fujita MK, Ruggiero RP, et al. The Burmese python
746 genome reveals the molecular basis for extreme adaptation in snakes. *Proceedings of the National
747 Academy of Sciences*. 2013;110(51):20645–20650. doi:10.1073/pnas.1324475110.
- 748 [59] Howe K, Clark MD, Torroja CF, Torrance J, Berthelot C, Muffato M, et al. The zebrafish refer-
749 ence genome sequence and its relationship to the human genome. *Nature*. 2013;496(7446):498–503.
750 doi:10.1038/nature12111.
- 751 [60] Amemiya CT, Alföldi J, Lee AP, Fan S, Philippe H, MacCallum I, et al. The African coelacanth genome
752 provides insights into tetrapod evolution. *Nature*. 2013;496(7445):311–316. doi:10.1038/nature12027.
- 753 [61] Smith JJ, Kuraku S, Holt C, Sauka-Spengler T, Jiang N, Campbell MS, et al. Sequencing of the sea
754 lamprey (*Petromyzon marinus*) genome provides insights into vertebrate evolution. *Nature genetics*.
755 2013;45(4):415–21, 421e1–2. doi:10.1038/ng.2568.
- 756 [62] Venkatesh B, Lee AP, Ravi V, Maurya AK, Lian MM, Swann JB, et al. Elephant shark genome provides
757 unique insights into gnathostome evolution. *Nature*. 2014;505(7482):174–179. doi:10.1038/nature12826.
- 758 [63] Zhang GG, Fang X, Guo X, Li L, Luo R, Xu F, et al. The oyster genome reveals stress adaptation
759 and complexity of shell formation. *Nature*. 2012;490(7418):49–54. doi:10.1038/nature11413.
- 760 [64] Keeling CI, Yuen MM, Liao NY, Roderick Docking T, Chan SK, Taylor Ga, et al. Draft genome of
761 the mountain pine beetle, *Dendroctonus ponderosae* Hopkins, a major forest pest. *Genome biology*.
762 2013;14(3):R27. doi:10.1186/gb-2013-14-3-r27.
- 763 [65] Richards S, Gibbs Ra, Weinstock GM, Brown SJ, Denell RE, Beeman RW, et al. The genome of the
764 model beetle and pest *Tribolium castaneum*. *Nature*. 2008;452(7190):949–55. doi:10.1038/nature06784.
- 765 [66] Mita K, Kasahara M, Sasaki S, Nagayasu Y, Yamada T, Kanamori H, et al. The genome sequence of
766 silkworm, *Bombyx mori*. *DNA research*. 2004;11:27–35.
- 767 [67] Nossa CW, Havlak P, Yue JX, Lv J, Vincent KY, Brockmann HJ, et al. Joint assembly and genetic
768 mapping of the Atlantic horseshoe crab genome reveals ancient whole genome duplication. *GigaScience*.
769 2014;3:9. doi:10.1186/2047-217X-3-9.
- 770 [68] The *C. elegans* Sequencing Consortium. Genome Sequence of the Nematode *C. elegans*: A Platform
771 for Investigating Biology. *Science*. 1998;282(5396):2012–2018. doi:10.1126/science.282.5396.2012.

- 772 [69] Sodergren E, Weinstock GM, Davidson EH, Cameron RA, Gibbs RA, Angerer RC, et al. The genome
773 of the sea urchin *Strongylocentrotus purpuratus*. *Science (New York, NY)*. 2006;314(5801):941–52.
774 doi:10.1126/science.1133609.
- 775 [70] Colbourne JK, Pfrender ME, Gilbert D, Thomas WK, Tucker A, Oakley TH, et al. The
776 ecoresponsive genome of *Daphnia pulex*. *Science (New York, NY)*. 2011;331(6017):555–61.
777 doi:10.1126/science.1197761.
- 778 [71] Weinstock GM, Robinson GE, Gibbs Ra, Worley KC, Evans JD, Maleszka R, et al. Insights into
779 social insects from the genome of the honeybee *Apis mellifera*. *Nature*. 2006;443(7114):931–949.
780 doi:10.1038/nature05260.
- 781 [72] Gulia-Nuss M, Nuss AB, Meyer JM, Sonenshine DE, Roe RM, Waterhouse RM, et al. Genomic
782 insights into the *Ixodes scapularis* tick vector of Lyme disease. *Nature Communications*. 2016;7(May
783 2015):10507. doi:10.1038/ncomms10507.
- 784 [73] Chipman AD, Ferrier DEK, Brena C, Qu J, Hughes DST, Schröder R, et al. The First Myriapod
785 Genome Sequence Reveals Conservative Arthropod Gene Content and Genome Organisation in the
786 Centipede *Strigamia maritima*. *PLoS Biology*. 2014;12(11). doi:10.1371/journal.pbio.1002005.
- 787 [74] Stanke M, Diekhans M, Baertsch R, Haussler D. Using native and syntenically mapped
788 cDNA alignments to improve de novo gene finding. *Bioinformatics*. 2008;24(5):637–644.
789 doi:10.1093/bioinformatics/btn013.
- 790 [75] Hoff KJ, Stanke M. WebAUGUSTUS—a web service for training AUGUSTUS and predicting genes in
791 eukaryotes. *Nucleic Acids Research*. 2013;41(W1):W123–W128. doi:10.1093/nar/gkt418.
- 792 [76] Chapman Ja, Kirkness EF, Simakov O, Hampson SE, Mitros T, Weinmaier T, et al. The dynamic
793 genome of *Hydra*. *Nature*. 2010;464(7288):592–6. doi:10.1038/nature08830.
- 794 [77] Kim D, Pertea G, Trapnell C, Pimentel H, Kelley R, Salzberg SL. TopHat2: accurate alignment of tran-
795 scriptomes in the presence of insertions, deletions and gene fusions. *Genome biology*. 2013;14(4):R36.
796 doi:10.1186/gb-2013-14-4-r36.
- 797 [78] Pertea M, Pertea GM, Antonescu CM, Chang TC, Mendell JT, Salzberg SL. StringTie enables im-
798 proved reconstruction of a transcriptome from RNA-seq reads. *Nature Biotechnology*. 2015;33(3).
799 doi:10.1038/nbt.3122.
- 800 [79] Preußner C, Jaé N, Bindereif A. mRNA splicing in trypanosomes. *International Journal of Medical*
801 *Microbiology*. 2012;302(4-5):221–224. doi:10.1016/j.ijmm.2012.07.004.
- 802 [80] Siegel TN, Hekstra DR, Wang X, Dewell S, Cross GAM. Genome-wide analysis of mRNA abundance
803 in two life-cycle stages of *Trypanosoma brucei* and identification of splicing and polyadenylation sites.
804 *Nucleic Acids Research*. 2010;38(15):4946–4957. doi:10.1093/nar/gkq237.
- 805 [81] Hardie DC, Hebert PD. Genome-size evolution in fishes. *Canadian Journal of Fisheries and Aquatic*
806 *Sciences*. 2004;61(9):1636–1646. doi:10.1139/f04-106.
- 807 [82] Treangen TJ, Salzberg SL. Repetitive DNA and next-generation sequencing: Computational challenges
808 and solutions. *Nature Reviews Genetics*. 2012;13(1):36–46. doi:10.1038/nrg3117.
- 809 [83] Kajitani R, Toshimoto K, Noguchi H, Toyoda A, Ogura Y, Okuno M, et al. Efficient de novo as-
810 sembly of highly heterozygous genomes from whole-genome shotgun short reads. *Genome Research*.
811 2014;24(8):1384–1395. doi:10.1101/gr.170720.113.
- 812 [84] Bankevich A, Nurk S, Antipov D, Gurevich Aa, Dvorkin M, Kulikov AS, et al. SPAdes: A New Genome
813 Assembly Algorithm and Its Applications to Single-Cell Sequencing. *Journal of Computational Biology*.
814 2012;19(5):455–477. doi:10.1089/cmb.2012.0021.

- 815 [85] Tilgner H, Nikolaou C, Althammer S, Sammeth M, Beato M, Valcárcel J, et al. Nucleosome positioning
816 as a determinant of exon recognition. *Nature structural & molecular biology*. 2009;16(9):996–1001.
817 doi:10.1038/nsmb.1658.
- 818 [86] Sakharkar MK, Chow VTK, Kanguene P. Distributions of exons and introns in the human genome.
819 *In silico biology*. 2004;4(4):387–93.
- 820 [87] Bellis ES, Howe DK, Denver DR. Genome-wide polymorphism and signatures of selection in the
821 symbiotic sea anemone *Aiptasia*. *BMC Genomics*. 2016;17:160. doi:10.1186/s12864-016-2488-6.
- 822 [88] Leffler EM, Bullaughey K, Matute DR, Meyer WK, S?gurel L, Venkat A, et al. Revisiting an
823 Old Riddle: What Determines Genetic Diversity Levels within Species? *PLoS Biology*. 2012;10(9).
824 doi:10.1371/journal.pbio.1001388.
- 825 [89] Bányai L, Patthy L. Putative extremely high rate of proteome innovation in lancelets might
826 be explained by high rate of gene prediction errors. *Scientific Reports*. 2016;6(April):30700.
827 doi:10.1038/srep30700.
- 828 [90] Zmasek CM, Godzik A. This Déjà Vu Feeling-Analysis of Multidomain Protein Evolution in Eukaryotic
829 Genomes. *PLoS Computational Biology*. 2012;8(11). doi:10.1371/journal.pcbi.1002701.
- 830 [91] Hahn MW, Wray GA. The g-value paradox. *Evolution and Development*. 2002;4(2):73–75.
831 doi:10.1046/j.1525-142X.2002.01069.x.
- 832 [92] Gregory TR. Synergy between sequence and size in large-scale genomics. *Nature reviews Genetics*.
833 2005;6(9):699–708. doi:10.1038/nrg1674.
- 834 [93] Denton JF, Lugo-Martinez J, Tucker AE, Schrider DR, Warren WC, Hahn MW. Extensive Error in the
835 Number of Genes Inferred from Draft Genome Assemblies. *PLoS Computational Biology*. 2014;10(12).
836 doi:10.1371/journal.pcbi.1003998.
- 837 [94] Fernandez-Valverde SL, Degnan BM. Bilaterian-like promoters in the highly compact *Amphimedon*
838 *queenslandica* genome. *Scientific Reports*. 2016;6(February):22496. doi:10.1038/srep22496.
- 839 [95] Wilson BA, Masel J. Putatively noncoding transcripts show extensive association with ribosomes.
840 *Genome biology and evolution*. 2011;3:1245–52. doi:10.1093/gbe/evr099.
- 841 [96] Slavoff Sa, Mitchell AJ, Schwaid AG, Cabili MN, Ma J, Levin JZ, et al. Peptidomic discovery of
842 short open reading frame-encoded peptides in human cells. *Nature chemical biology*. 2012;9(1):59–64.
843 doi:10.1038/nchembio.1120.
- 844 [97] Guttman M, Russell P, Ingolia NT, Weissman JS, Lander ES. Ribosome profiling pro-
845 vides evidence that large noncoding RNAs do not encode proteins. *Cell*. 2013;154(1):240–251.
846 doi:10.1016/j.cell.2013.06.009.
- 847 [98] Petrov D. Mutational Equilibrium Model of Genome Size Evolution. *Theoretical Population Biology*.
848 2002;61(4):531–544. doi:10.1006/tpbi.2002.1605.
- 849 [99] Moore G. The C-Value Paradox. *BioScience*. 1984;34(7):425–429. doi:10.2307/1309631.
- 850 [100] Thiébaud CH, Fischberg M. DNA content in the genus *Xenopus*. *Chromosoma*. 1977;59(3):253–7.
- 851 [101] Schad E, Tompa P, Hegyi H. The relationship between proteome size, structural disorder and organism
852 complexity. *Genome biology*. 2011;12(12):R120. doi:10.1186/gb-2011-12-12-r120.
- 853 [102] Nilsen TW, Graveley BR. Expansion of the eukaryotic proteome by alternative splicing. *Nature*.
854 2010;463(January). doi:10.1038/nature08909.
- 855 [103] Brett D, Pospisil H, Valcárcel J, Reich J, Bork P. Alternative splicing and genome complexity. *Nature*
856 *genetics*. 2002;30(1):29–30. doi:10.1038/ng803.

- 857 [104] Kim H, Klein R, Majewski J, Ott J. Estimating rates of alternative splicing in mammals and invertebrates. *Nature genetics*. 2004;36(9):915–6; author reply 916–7. doi:10.1038/ng0904-915.
858
- 859 [105] Chen L, Bush SJ, Tovar-Corona JM, Castillo-Morales A, Urrutia AO. Correcting for differential transcript coverage reveals a strong relationship between alternative splicing and organism complexity. *Molecular biology and evolution*. 2014;31(6):1402–13. doi:10.1093/molbev/msu083.
860
861
- 862 [106] Kim E, Magen A, Ast G. Different levels of alternative splicing among eukaryotes. *Nucleic Acids Research*. 2007;35(1):125–131. doi:10.1093/nar/gkl924.
863
- 864 [107] Pickrell JK, Pai AA, Gilad Y, Pritchard JK. Noisy splicing drives mRNA isoform diversity in human cells. *PLoS Genetics*. 2010;6(12):1–11. doi:10.1371/journal.pgen.1001236.
865
- 866 [108] Jeffery NW, Jardine CB, Gregory TR. A first exploration of genome size diversity in sponges. *Genome*. 2013;56(8):451–6. doi:10.1139/gen-2012-0122.
867
- 868 [109] Gregory TR, Andrews CB, McGuire JA, Witt CC. The smallest avian genomes are found in hummingbirds. *Proceedings Biological sciences / The Royal Society*. 2009;276(1674):3753–3757. doi:10.1098/rspb.2009.1004.
869
870
- 871 [110] Consortium ME. A comparative encyclopedia of DNA elements in the mouse genome. *Nature*. 2014;515(7527):355–364. doi:10.1038/nature13992.
872
- 873 [111] van Bakel H, Nislow C, Blencowe BJ, Hughes TR. Most "dark matter" transcripts are associated with known genes. *PLoS Biology*. 2010;8(5). doi:10.1371/journal.pbio.1000371.
874
- 875 [112] Clark MB, Amaral PP, Schlesinger FJ, Dinger ME, Taft RJ, Rinn JL, et al. The reality of pervasive transcription. *PLoS Biology*. 2011;9(7):5–10. doi:10.1371/journal.pbio.1000625.
876
- 877 [113] Nóbrega MA, Zhu Y, Plajzer-Frick I, Afzal V, Rubin EM. Megabase deletions of gene deserts result in viable mice. *Nature*. 2004;431(7011):988–93. doi:10.1038/nature03022.
878